# Deconvolution Over Groups in Image Reconstruction*

BIRSEN YAZICI AND CAN EVREN YARMAN

*Department of Electrical, Computer and Systems Engineering, Rensselaer Polytechnic Institute, Troy, New York 12180, USA*



* **Disclaimer**
The views and conclusions contained herein are those of the authors and should not be interpreted as necessarily representing the official policies or endorsements, either expressed or implied, of the Air Force Research Laboratory or the U.S. Government.



ISSN 1076-5670/05
DOI: 10.1016/S1076-5670(05)41004-6

# I. Introduction

## A. Motivations

Convolution integrals over groups arise in a broad array of science and engineering problems. This is due to the ubiquitous presence of *invariance* or *symmetry* in natural and man-made systems. Many imaging systems, for example, have symmetry properties. These include an ordinary circular lens that exhibits rotational invariance with respect to its optical axis and a X-ray tomographic system that exhibits invariance with respect to rigid body motions of the Euclidean space. The mathematical framework that underlies the concept of invariance is group theory. This chapter describes a group theoretic framework for system modeling and signal processing to describe and exploit invariance. We then apply this framework to two image reconstruction problems formulated as convolution integrals over groups.

The discussion starts with the review of the group theoretic signal and system theory introduced in Yazici (2004) and shows how group theory leads to expanded understanding of familiar concepts such as convolution, Fourier analysis, and stationarity. Group convolution operation is defined as a representation of the input–output relationship of a linear system, which has dynamics invariant under the group composition law. Fourier transforms over groups are introduced to study convolution operation that transforms convolution to operator multiplication in the Fourier domain. The concept of group stationarity, generalizing ordinary stationarity, is introduced to model imperfect symmetries. Spectral decomposition of group stationary processes is presented using Fourier transforms over groups. *Deconvolution problem* over groups is introduced, and a review of the Wiener-type minimum mean square error solution to the deconvolution problem is presented.

Next, this group-theoretic framework is applied to address two imaging problems: (1) target estimation in wideband extended range-Doppler imaging and diversity waveform design and (2) inversion of the Radon and exponential Radon transforms for transmission and emission tomography.

In the first problem, the output of the match filter becomes convolution integral over the affine or Heisenberg group, depending on whether the underlying model is wideband or narrowband. However, for the wideband model, modeling the received echo as the Fourier transform of the reflectivity density function over the affine group allows implementation of the Wiener-type deconvolution in the Fourier transform domain. Therefore, the echo model is modeled as the Fourier transform of the superposition of the target and unwanted scatterers. The receiver and waveform design problems are addressed within the Wiener filtering framework defined over the affine group. The approach allows joint design of adaptive transmit and receive methods for wideband signals.

In the second problem, both Radon and exponential Radon transforms are formulated as convolutions over the Euclidean motion group of the plane. Hence, recovering a function from its Radon or exponential Radon transform projections becomes a deconvolution problem over the Euclidean motion group. The deconvolution is performed by applying a special case of the Wiener filter introduced in Section IV. The approach presented for the Radon and exponential Radon transform can be extended to other integral transforms of transmission and emission tomography, unifying them under a single convolution representation (Yarman and Yazici, 2005e).

Apart from these imaging problems, convolutions over groups appear in a broad array of engineering problems. These include workspace estimation in robotics, estimation of the structure of macromolecules in polymer science, estimation of illumination and bidirectional reflectance distribution function in computer graphics, and motion estimation in omnidirectional vision (Blahut, 1991; Chirikjian and Ebert-Uphoff, 1998; Ebert-Uphoff and Chirikjian, 1996; Ferraro, 1992; Kanatani, 1990; Lenz, 1990; Miller, 1991; Naparst, 1991; Popplestone, 1984; Ramamoorthi and Hanrahan, 2001; Srivastava and Buschman, 1977; Volchkov, 2003).

### *B. Organization*

Section II introduces the concept of convolution and Fourier analysis over groups. Section III presents stochastic processes exhibiting invariance with respect to group composition law and their spectral decomposition theorems. Section IV describes Wiener filtering over groups as a solution of the deconvolution problem. Section V addresses wideband target estimation and waveform design problems. Section VI presents the inversion of Radon and exponential Radon transforms of transmission and emission tomography within the framework introduced in Sections II to IV.

## II. Convolution and Fourier Analysis on Groups

Let $G$ be a group. We denote the composition of two elements $g, h \in G$ by $gh$, the identity element by $e$ (i.e., $eg = ge = g$, for all $g \in G$), and inverse of an element $g$ by $g^{-1}$ (i.e., $g^{-1}g = gg^{-1} = e$). It is assumed that the reader is familiar with the concepts of group theory and topological spaces. For an introduction to group theory and topological groups, the reader is referred to Sattinger and Weaver (1986) and Artin (1991).

### A. Convolution on Groups

Recall that the input–output relationship of a linear time-invariant system can be represented as a convolution integral

$$(f_{\text{in}} * \Lambda)(t) \equiv f_{\text{out}}(t) = \int_{-\infty}^{\infty} f_{\text{in}}(\tau)\Lambda(t-\tau)\, d\tau. \tag{1}$$

The fundamental property of the ordinary convolution integral is its invariance under time shifts. To generalize ordinary convolution to functions over groups, an appropriate integration measure invariant under group translations must be defined:

$$\int_G f(g)\, d\mu(g) = \int_G f(hg)\, d\mu(g), \tag{2}$$

for all $h$ in $G$ and integrable $f$. For locally compact groups, such an integration measure exists and is called the *left Haar measure*. Left Haar measure satisfies $d\mu(hg) = d\mu(g)$, while *right Haar measure* satisfies $d\mu_R(gh) = d\mu_R(g)$. In general, left and right Haar measures are not equal for an arbitrary group. However, one has $d\mu_R(g) = \Delta^{-1}(g)\, d\mu(g)$, where $\Delta(g)$ is the *modular function* satisfying $\Delta(e) = 1$, $\Delta(g) > 0$, $\Delta(gh) = \Delta(g)\Delta(h)$. Those groups for which the modular function is 1 are called *unimodular*. For example, the Euclidean motion group and the Heisenberg group are unimodular, but affine and scale Euclidean groups are nonunimodular.

Results involving the right Haar measure can be easily deduced from the results associated with the left Haar measure. Therefore, for the remainder of this chapter, unless stated otherwise, we shall use the left Haar measure and denote it by $dg$.

Let $L^2(G, dg)$ denote the Hilbert space of all complex-valued, square-integrable functions on the group $G$, that is, $f \in L^2(G, dg)$, if

$$\int_G |f(g)|^2\, dg < \infty. \tag{3}$$

Let $f_{\text{in}}, f_{\text{out}} \in L^2(G, dg)$ be two signals, representing the input and output of a linear system $\mathcal{S}$, that is, $\mathcal{S}[f_{\text{in}}(g)] = f_{\text{out}}(g)$. If $\mathcal{S}$ has the following group invariant property

$$\mathcal{S}\big[f_{\text{in}}(hg)\big] = f_{\text{out}}(hg), \tag{4}$$

for all $g, h \in G$, then the input–output relationship between $f_{\text{in}}$ and $f_{\text{out}}$ reduces to a *convolution* over the group $G$ and is given as

$$(f_{\text{in}} * \Lambda)(g) \equiv f_{\text{out}}(g) = \int_G f_{\text{in}}(h)\Lambda\big(h^{-1}g\big)\, dh. \tag{5}$$

Here, we refer to $\Lambda$ as the kernel or the *impulse response function* of the linear system $\mathcal{S}$.

Note that the convolution operation is not necessarily commutative for noncommutative groups.

For a function $f$ on $G$, $f(h^{-1}g)$ is called a translation of $f$ by $h$, in the same sense that $f(t - \tau)$ is a translation of a function on $\mathbb{R}$ by $\tau$. In particular, $[L(h)f](g) = f(h^{-1}g)$ is called a *left regular representation*, while $[R(h)f](g) = f(gh)$ is called a *right regular representation* of the group over $L^2(G, dg)$.

Convolution integral can also be expressed in terms of the left regular representation of the group

$$(f * \Lambda)(g) = \langle f, L(g)\Lambda^* \rangle = \big\langle L\big(g^{-1}\big) f, \Lambda^* \big\rangle, \tag{6}$$

where $\Lambda^*(g) = \overline{\Lambda(g^{-1})}$, $\overline{\Lambda}$ being the complex conjugate of $\Lambda$, and $\langle \cdot, \cdot \rangle$ is the inner product on $L^2(G, dg)$ defined as

$$\langle f, \Lambda \rangle = \int_G f(h)\overline{\Lambda(h)}\, dh. \tag{7}$$

Let $X$ be a homogeneous space of $G$, that is, $gX = X$. Then, convolution operation over homogeneous spaces is obtained by replacing the left regular representation in Eq. (6) with the *quasi-left regular representation*:

$$f_{\text{out}}(g) = \big\langle L_q\big(g^{-1}\big) f_{\text{in}}, \Lambda^* \big\rangle, \tag{8}$$

where $\Lambda$ and $f_{\text{in}}$ are elements of $L^2(X)$ and $L_q(g) f_{\text{in}}(t) = f_{\text{in}}(g^{-1}t)$.

Note that both the echo signal in radar/sonar imaging and the tomographic imaging process described in Sections V and VI can be viewed as convolution operations over homogeneous spaces.

### B. Fourier Analysis on Groups

Fourier analysis on groups allows spectral analysis of signals and system in invariant subspaces determined by the irreducible unitary representations of the underlying group. This requires characterization of the unitary representations, which in return leads to the definition of the Fourier transforms on groups. It was shown that if the group $G$ is a separable, locally compact group of Type I, unique characterizations of the unitary representations can be obtained in terms of the irreducible unitary representations of the group (Naimark, 1959). This class of groups include finite, compact, and algebraic Lie groups, separable locally compact commutative groups, and the majority of well-behaved locally compact groups. Many of the groups involved in engineering applications, such as the affine group, the Heisenberg group, and Euclidean motion group, fall into this class of groups.

The following text provides a review of the Fourier analysis on locally compact groups of Type I for both unimodular and nonunimodular case. Definitions of the basic concepts in group representation theory are provided in Appendix A. For a detailed discussion of the topic, the reader is referred to Groove (1997), Milies and Sehgal (2002), and Onishchik (1993).

Let $U(g, \lambda)$ be the $\lambda$th irreducible unitary representation of a separable locally compact group of Type I. Then, the operator valued *Fourier transform* on $G$ maps each $f$ in $L^2(G, dg)$ to a family $\{\hat{f}(\lambda)\}$ of bounded operators, where each $\hat{f}(\lambda)$ is defined as

$$\mathcal{F}(f)(\lambda) \equiv \hat{f}(\lambda) = \int_G dg f(g) U\big(g^{-1}, \lambda\big), \tag{9}$$

or in component form

$$\hat{f}_{i,j}(\lambda) = \int_G f(g) U_{i,j}\big(g^{-1}, \lambda\big)\, dg, \tag{10}$$

where $\hat{f}_{i,j}(\lambda)$ and $U_{i,j}(g, \lambda)$ denote the $(i, j)$th matrix elements of $\hat{f}(\lambda)$ and $U(g, \lambda)$, respectively. The collection of all $\lambda$ values is denoted by $\widehat{G}$ and is called the *dual* of the group $G$. The collection of Fourier transforms $\{\hat{f}(\lambda)\}$ for all $\lambda \in \widehat{G}$ is called the *spectrum* of the function $f$. The Fourier transform is a one-to-one onto transformation from $L^2(G, dg)$ to $L^2(\widehat{G}, d\nu(\lambda))$, where $d\nu(\lambda)$ denotes the *Plancherel* measure in $\widehat{G}$.

An important property of the operator-valued Fourier transform is that the group convolution becomes operator multiplication in the Fourier domain

$$\mathcal{F}(f_1 * f_2)(\lambda) = \mathcal{F}(f_2)(\lambda)\mathcal{F}(f_1)(\lambda). \tag{11}$$

For the case of separable locally compact groups of Type I, the Fourier inversion and the Plancherel formulas are given by Duflo and Moore (1976):

$$f(g) = \int_{\widehat{G}} \operatorname{trace}\big(\big[\hat{f}(\lambda)\xi_\lambda^{-2}\big]U^\dagger(g,\lambda)\big)\,d\nu(\lambda), \tag{12}$$

and

$$\int_G \big|f(g)\big|^2\,dg = \int_{\widehat{G}} \operatorname{trace}\big(\big[\hat{f}(\lambda)\xi_\lambda^{-1}\big]\big[\hat{f}(\lambda)\xi_\lambda^{-1}\big]^\dagger\big)\,d\nu(\lambda), \tag{13}$$

where $\hat{f}^\dagger(\lambda)$ denotes the adjoint of $\hat{f}(\lambda)$ and $\{\xi_\lambda\}$ is a family of Hermitian positive definite operators with densely defined inverses satisfying the following conditions:

- $\{\hat{f}(\lambda)\xi_\lambda\}$ is trace class for each $\lambda \in \widehat{G}$ and
- $U(g,\lambda)\xi_\lambda U^\dagger(g,\lambda) = \Delta^{1/2}(g)\xi_\lambda$

where $\Delta(g)$ is the modular function of the group $G$.

For a given locally compact group of Type I, both the family of operators $\{\xi_\lambda\}$ and the Plancherel measure can be determined uniquely. When the group is unimodular, $\xi_\lambda = I_\lambda$, $I_\lambda$ being the identity operator. Thus, the Fourier inversion and the Plancherel formulas become

$$f(g) = \int_{\widehat{G}} \operatorname{trace}\big(\hat{f}(\lambda)U^\dagger(g,\lambda)\big)\,d\nu(\lambda), \tag{14}$$

and

$$\int_G \big|f(g)\big|^2\,dg = \int_{\widehat{G}} \operatorname{trace}\big(\hat{f}(\lambda)\hat{f}^\dagger(\lambda)\big)\,d\nu(\lambda). \tag{15}$$

In the following section, Fourier transform is used to develop spectral decomposition theorems for a class of nonstationary stochastic processes.

## III. Group Stationary Processes

One of the key components of our development is the generalized second-order stationary processes indexed by topological groups (Diaconis, 1988; Hannan, 1965; Yaglom, 1961). These processes are nonstationary in the classical sense but exhibit invariance under the right or left regular transformations of the group.

Let $G$ denote a group and $g, h$ be its elements. Then, we call a process $X(g)$, $g \in G$, *group stationary* if

$$X(g) \equiv X(hg), \quad g, h \in G, \tag{16}$$

or

$$X(g) \equiv X(gh), \quad g, h \in G, \tag{17}$$

where $\equiv$ denotes equality in terms of all finite joint probability distributions of $\{X(g), g \in G\}$. Depending on whether a random process satisfies Eq. (16), Eq. (17), or both, it is called *left*, *right*, or *two-way* group stationary. Note that for commutative groups, the process is always two-way group stationary.

Second-order group stationarity is a weaker condition than group stationarity. A process $X(g)$, $g \in G$, is said to be *second-order right group stationary* if

$$E\big[X(g)\overline{X(h)}\,\big] = R\big(gh^{-1}\big), \quad g, h \in G, \tag{18}$$

and *second-order left group stationary* if

$$E\big[X(g)\overline{X(h)}\,\big] = R\big(h^{-1}g\big), \quad g, h \in G, \tag{19}$$

where $R$ is a positive definite function defined on the group $G$. We shall refer to $R$ as the autocorrelation function of $X(g)$, $g \in G$. A process is called *second-order group stationary* if it is both left and right stationary.

The central fact in the analysis of group stationary processes is the existence of the spectral decomposition, which is facilitated by the group representation theory. For separable locally compact groups of Type I, the left group stationary processes admit the following spectral decomposition:

$$X(g) = \int_{\widehat{G}} \operatorname{trace}\big(U(g, \lambda)Z(d\lambda)\big), \tag{20}$$

and

$$R(g) = \int_{\widehat{G}} \operatorname{trace}\big(U(g, \lambda)F(d\lambda)\big), \tag{21}$$

where $R$ is the autocorrelation function defined in Eq. (19), $Z(d\lambda)$ is a random linear operator over $\widehat{G}$, and $F(d\lambda)$ is an operator measure over $\widehat{G}$ satisfying

$$\int_{\widehat{G}} \operatorname{trace}\big(F(d\lambda)\big) < \infty. \tag{22}$$

Unless the process is both right and left group stationary, the matrix entries of the random linear operator $Z(\cdot)$ is column-wise correlated and row-wise uncorrelated with correlation coefficients equal to the corresponding matrix entries of the operator $F(\cdot)$. For a detailed discussion of the topic, refer to Yaglom (1961) and Hannan (1965).

Now, let us assume that the autocorrelation function $R \in L^2(G, dg)$. We define the *spectral density function* $S$ of a group stationary process as

$$S(\lambda) \equiv \mathcal{F}(R)(\lambda) = \int_G dg R(g) U(g, \lambda). \tag{23}$$

For unimodular groups, $S$ is a bounded nonnegative definite operator, defined on the dual space $\widehat{G}$. For nonunimodular groups, $S$ can be modified to $\widetilde{S} = S\xi$, so that the resulting operator is Hermitian, nonnegative definite. The spectral density function represents the correlation structure of the random linear operators $Z(\cdot)$.

Some examples of group stationary processes are provided below.

1. *Shift Stationary Processes*

The simplest example is the ordinary stationary processes defined on the real line with the addition operation, that is, the additive group $(\mathbb{R}, +)$,

$$E\left[X(t_1)\overline{X(t_2)}\right] = R(t_1 - t_2), \quad -\infty < t_1, t_2 < \infty. \tag{24}$$

One-dimensional irreducible unitary representations of the additive group $(\mathbb{R}, +)$ are given by the complex exponential functions $e^{i\omega t}$, $-\infty < t_1$, $t_2 < \infty$. Hence, the spectral decomposition of the shift stationary processes is given by the ordinary Fourier transform.

2. *Scale Stationary Processes*

Another important class of group stationary processes is defined by the multiplicative group, on the positive real line, that is, $(\mathbb{R}^+, \times)$. These processes exhibit invariance with respect to translation in scale and are referred to as *scale stationary processes* (Yazici and Kashyap, 1997). Their autocorrelation function satisfies the following invariance property:

$$E\left[X(t_1)\overline{X(t_2)}\right] = R(t_1/t_2), \quad 0 < t_1, t_2 < \infty. \tag{25}$$

One-dimensional irreducible unitary representations of the multiplicative group are given by $e^{i\omega \log t}$, $t > 0$. As a result, the spectral decomposition of the scale stationary processes is given by the Mellin transform. Detailed analysis of the self-similar processes based on the concept of scale stationarity can be found in the first author's previous works (Yazici, 1997; Yazici and Izzetoglu, 2002; Yazici *et al.*, 2001; Yazici and Kashyap, 1997).

3. *Filtered White Noise*

A trivial group stationary process is the *white noise* process with autocorrelation function given by $\sigma^2\delta(g)$, $g \in G$, where $\sigma^2$ denotes the variance of the process. Here, $\delta(g)$ is the Dirac delta function over the group $G$, supported at the identity element and has its integral over $G$ equal to one. It was shown in Yazici (2004) that the convolution of white noise process with any $f \in L^2(G, dg)$ leads to a second-order left group stationary process.

Apart from these examples, detailed discussions on stochastic processes invariant with respect to multiplicative group, affine group, and two- and three-dimensional rotational group action can be found in Yazici and Kashyap (1997), Yazici (1997, 2004), Yazici *et al.* (2001), Yazici and Izzetoglu (2002), Yadrenko (1983), and Tewfik (1987) and references therein.

## IV. Wiener Filtering Over Groups

In Yazici (2004), we introduced a deconvolution method over locally compact groups of Type I. This section provides a review of this method.

Let $\mathcal{S}$ be a left group invariant system defined on a locally compact group $G$ of Type I, and let $f_{\text{out}}$ be the noisy output of the system for an input $f_{\text{in}}$, given by the following convolution integral:

$$f_{\text{out}}(g) = \int_G f_{\text{in}}(h)\Lambda\left(h^{-1}g\right)dh + n(g), \tag{26}$$

where $\Lambda : G \to \mathbb{C}$ is the complex-valued, square-summable impulse response function of the group invariant system $\mathcal{S}$, $f_{\text{in}}$ is the unknown signal, and $n$ is the additive noise. Both $f_{\text{in}}$ and $n$ are left group stationary and take values in the field of complex numbers $\mathbb{C}$.

Without loss of generality, we assume that $E[f_{\text{in}}(g)] = E[n(g)] = 0$ and that $f_{\text{in}}$ and $n$ are uncorrelated, that is,

$$E\left[f_{\text{in}}(g)\overline{n(g)}\right] = 0. \tag{27}$$

Our objective is to design a linear filter $W$ on $G \times G$ to estimate $f_{\text{in}}$, that is,

$$\tilde{f}_{\text{in}}(g) = \int_G W(g,h) f_{\text{out}}(h)\,dh, \tag{28}$$

given the measurements $f_{\text{out}}$, systems response function $\Lambda$, and a priori statistical information on $f_{\text{in}}$ and $n$.

Under stationary assumption, it can be shown that $W(hg_1, hg_2) = W(g_1, g_2)$ for all $g_1, g_2, h \in G$. Therefore, the estimate of $\tilde{f}_{\text{in}}$ of the signal

$f_{\text{in}}$ is given as the following convolution integral:

$$\tilde{f}_{\text{in}}(g) = \int_G f_{\text{out}}(h) W\big(h^{-1}g\big)\, dh, \tag{29}$$

where $W(g) = W(g, e)$.

Let $\varepsilon_W(g) = \tilde{f}_{\text{in}}(g) - f_{\text{in}}(g)$. We design the filter $W$ so that the mean square error

$$\int_G E\Big[\big|\varepsilon_W(g)\big|^2\Big]\, dg, \tag{30}$$

is minimized. It can be shown that the Fourier transform of the minimum mean square error (MMSE) deconvolution filter $W_{\text{opt}}$ is given by

$$\widehat{W}_{\text{opt}}(\lambda) = S_{f_{\text{in}}}(\lambda)\widehat{\Lambda}^{\dagger}(\lambda)\Big[\widehat{\Lambda}(\lambda)S_{f_{\text{in}}}(\lambda)\widehat{\Lambda}^{\dagger}(\lambda) + S_n(\lambda)\Big]^{-1}, \quad \lambda \in \widehat{G}. \tag{31}$$

Here, $\widehat{\Lambda}$ is the Fourier transform of the convolution filter $\Lambda$, and $\widehat{\Lambda}^{\dagger}$ denotes the adjoint of the operator $\widehat{\Lambda}$. $S_{f_{\text{in}}}$ and $S_n$ are operator-valued spectral density functions of the signal and noise, respectively.

The spectral density function of the MMSE between the signal and its filtered estimate is given by

$$S_{\varepsilon}(\lambda) = \big(I - \widehat{W}_{\text{opt}}(\lambda)\widehat{\Lambda}(\lambda)\big) S_{f_{\text{in}}}(\lambda), \tag{32}$$

where $I$ denotes the identity operator. For the derivation of the Wiener filter stated above, we refer the reader to Theorem 2 in Yazici (2004).

### *A. Remarks*

The Fourier domain inverse filtering can be summarized by the following diagram:

$$\begin{array}{ccc} f_{\text{in}} & \xrightarrow{\Lambda} & f_{\text{out}} \\ \mathcal{F}^{-1}\uparrow & & \downarrow\mathcal{F} \\ \widehat{f_{\text{in}}} & \xleftarrow[\widehat{W}_{\text{opt}}]{} & \widehat{f_{\text{out}}} \end{array}. \tag{33}$$

Note that $\widehat{\Lambda}(\lambda)S_{f_{\text{in}}}(\lambda)\widehat{\Lambda}^{\dagger}(\lambda) + S_n(\lambda)$ is a nonnegative definite operator. Thus, its inverse exists but may be unbounded. In that case, $[\widehat{\Lambda}(\lambda)S_{f_{\text{in}}}(\lambda)\widehat{\Lambda}^{\dagger}(\lambda) + S_n(\lambda)]^{-1}$ can be interpreted as the pseudo-inverse.

Similar to the classical Wiener filtering, the results stated above can be extended to the case where the signal and the noise are correlated (Yazici, 2004).

Note that the proposed Wiener filter provides a regularized solution to the inversion problem. With appropriate choice of prior and noise model, one can ensure that $\widehat{\Lambda}(\lambda)S_{f_{\text{in}}}(\lambda)\widehat{\Lambda}^{\dagger}(\lambda) + S_n(\lambda)$ is a positive definite operator with eigenvalues away from zero.

If a priori information on the unknown signal is not available, it can be assumed that $S_{f_{\text{in}}}(\lambda) = I(\lambda)$. Furthermore, when the measurements are free of noise, the Wiener filter becomes the minimum norm linear least squares filter given by

$$\widehat{W}_{\text{opt}}(\lambda) = \widehat{\Lambda}^{\dagger}(\lambda)\big[\widehat{\Lambda}(\lambda)\widehat{\Lambda}^{\dagger}(\lambda)\big]^{-1}. \tag{34}$$

However, if $\widehat{\Lambda}(\lambda)$ is compact, this estimate is unstable in the sense that small deviations in measurements lead to large fluctuations in the estimation. The zero-order Tikhonov regularization (Tikhonov and Arsenin, 1977) of the form

$$\widehat{W}_{\text{opt}}(\lambda) = \widehat{\Lambda}^{\dagger}(\lambda)\big[\widehat{\Lambda}(\lambda)\widehat{\Lambda}^{\dagger}(\lambda) + \sigma^2 I(\lambda)\big]^{-1} \tag{35}$$

is equivalent to the case when $S_{f_{\text{in}}}(\lambda) = I(\lambda)$ and $S_n(\lambda) = \sigma^2 I(\lambda)$.

Note that in Kyatkin and Chirikjian (1998), Chirikjian *et al.* provided Eq. (35) as a solution to the convolution equation over the Euclidean motion groups, which is a special case of the proposed Wiener filtering method.

In the next two sections, we introduce two image reconstruction problems, namely wideband extended range-Doppler imaging for radar/sonar and inversion of Radon and exponential Radon transforms for transmission and emission tomography. Both problems are addressed within the Wiener filtering framework introduced in Sections II to IV.

## V. Wideband Extended Range-Doppler Imaging

In radar/sonar imaging, the transmitter emits an electromagnetic signal. The signal is reflected off a target and detected by the receiver as the echo signal. Assuming negligible acceleration of the reflector, the echo model from a point reflector is given as the delayed and scaled replica of the transmitted pulse $p$ (Cook and Bernfeld, 1967; Miller, 1991; Swick, 1969; Weiss, 1994)

$$e(t) = \sqrt{s}\, p\big(s(t-\tau)\big), \tag{36}$$

where $\tau$ is the time delay and $s$ is the time scale or Doppler stretch. The term $s$ is given as $s = \frac{c-v}{c+v}$, where $c$ is the speed of the transmitted signal and $v$ is the radial velocity of the reflector. When the transmitted signal is narrowband, the above echo model Eq. (36) can be approximated as

$$e(t) = p(t-\tau)\, \mathrm{e}^{\mathrm{i}\omega t}, \tag{37}$$

where $\omega$ is called the Doppler shift. In general, Eq. (36) is referred to as the *wideband* echo model and Eq. (37) is referred to as the *narrowband* echo model. The narrowband model is sufficient for most radar applications. However, for sonar and ultrawideband radar, the wideband model is needed (Taylor, 1995).

It is often desirable to image a dense group of reflectors. This means that the target environment is composed of several objects or a physically large object with a continuum of reflectors and that the reflectors are very close in range-Doppler space. This dense group of reflectors is described by a *reflectivity density function* in the range-Doppler space. The received signal is modeled as a weighted average (Blahut, 1991; Miller, 1991; Naparst, 1991) of the time delayed and scaled version of the transmitted pulse. For wideband signals, the echo model is given as

$$e(t) = \int_{-\infty}^{\infty} \int_{0}^{\infty} T_W(s, \tau) \frac{1}{\sqrt{s}} p\left(\frac{t-\tau}{s}\right) \frac{ds}{s^2}\, d\tau, \tag{38}$$

where $T_W$ is the *wideband reflectivity density function* associated with each time delayed and scaled version of the transmitted signal $p$. For narrowband, the echo model is given as

$$e(t) = \int_{-\infty}^{\infty} T_N(\omega, \tau) p(t-\tau)\, \mathrm{e}^{\mathrm{i}\omega t}\, d\tau\, d\omega, \tag{39}$$

where $T_N(\omega, \tau)$ is the *narrowband reflectivity density function* associated with each time-delayed and frequency-shifted version of the transmitted signal $p$.

Note that, for wideband signals, the output of the match filter becomes a convolution integral over the affine group

$$A_c(s, \tau) = \int_{-\infty}^{\infty} \int_{0}^{\infty} T_W(a, b) \frac{1}{\sqrt{s}} A_a\left(\frac{s}{a}, \frac{\tau - b}{a}\right) \frac{da}{a^2}\, db, \tag{40}$$

where $A_c$ denotes the cross-ambiguity function and $A_a$ denotes the auto-ambiguity function (Miller, 1991).

In general, the received echo is contaminated with clutter and noise. Here, we model clutter as an echo signal from unwanted scatterers and noise as the thermal noise. Therefore, the received signal is modeled as

$$y(t) = e_T(t) + e_C(t) + n(t), \tag{41}$$

where $n(t)$ is the thermal noise, $e_T(t)$ is the echo signal from the target modeled as in Eq. (38), and $e_C(t)$ is the echo signal from the clutter modeled

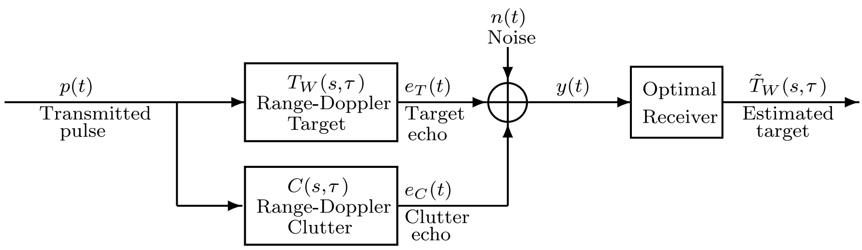


FIGURE 1. A block diagram of the range-Doppler echo model.

as

$$e_C(t) = \int_{-\infty}^{\infty} \int_{0}^{\infty} C(s,t) \frac{1}{\sqrt{s}} p\left(\frac{t-\tau}{s}\right) \frac{ds}{s}\, d\tau. \tag{42}$$

Here, we refer $C$ as the clutter reflectivity density function. Figure 1 displays the components of the radar/sonar range-Doppler echo model.

The goal in range-Doppler imaging is to estimate $T_W(a,b)$ given the transmitted and received signals and clutter, noise, and target statistics. Clearly, the transmitted pulse plays a central role in the estimation of the target reflectivity density function.

The two fundamental problems addressed in this chapter can be summarized as follows:

1. *Receiver design problem*. How can we recover the wideband target reflectivity density function $T_W$ in range-Doppler space from the measurements $y(t)$, $t \in \mathbb{R}$, embedded in clutter given a priori target and clutter information?
2. *Waveform design problem*. Given the echo model embedded in clutter, what is the best set of waveforms to transmit for the optimal recovery of the target reflectivity density function given the prior information on the target and background clutter?

The wideband model as described in Eq. (38) has been studied before. (See, Miller, 1991; Cook and Bernfeld, 1967; Swick, 1969; Weiss, 1994; Naparst, 1991; Rebollo-Neira *et al.*, 1997, 2000 and references therein.) Naparst (1991) and Miller (1991) suggested the use of the Fourier theory of the affine group and proposed a method to reconstruct the target reflectivity density function in a deterministic setting. Weiss (1994) suggested use of the wavelet transform for the image recovery in a deterministic setting. However, this approach requires target reflectivity function to be in the reproducing kernel Hilbert space of the transmitted wavelet signal. In Rebollo-Neira *et al.* (1997, 2000), the approach in Weiss (1994) is extended to include affine frames. In all these studies, the received signal is modeled clutter and noise free, which is not a realistic assumption for radar or sonar measurements.

Our approach is based on the observation that the received echo can be treated as the Fourier transform of the reflectivity density function evaluated at the transmitted pulse. We model target and clutter reflectivity as stationary processes on the affine group and use the Wiener filtering approach presented in Section IV to remove clutter by transmitting clutter rejecting waveforms.

Our treatment starts with the review of the affine group and its Fourier transform. Next, we discuss the estimation of target reflectivity function and design of clutter rejecting waveforms. Note that this study does not address the suppression of additive noise. For the treatment of this case, see Yazici and Xie (2005).

### *A. Fourier Theory of the Affine Group*

#### 1. *Affine Group*

Affine group or the $ax+b$ group is a two-parameter Lie group whose elements are given by $2 \times 2$ matrices of the form

$$\begin{bmatrix} a & b \\ 0 & 1 \end{bmatrix}, \quad a \in \mathbb{R}^+,\ b \in \mathbb{R}, \tag{43}$$

parameterized by the scale parameter $a$ and the translation parameter $b$.

The affine group operation is the usual matrix multiplication, that is, $(a, b)(c, d) = (ac, ad + b)$, and the inverse elements are given by the matrix inversion $(a, b)^{-1} = (a^{-1}, -a^{-1}b)$. This defines the affine group as a semidirect product of the additive group $(\mathbb{R}, +)$ and the multiplicative group $(\mathbb{R}^+, \times)$. For the rest of the chapter, the affine group is denoted by $\mathbb{A}$.

Let $(s, \tau) \in \mathbb{A}$, and let $L^2(\mathbb{A}, s^{-2}\, ds\, d\tau)$ and $L^1(\mathbb{A}, s^{-2}\, ds\, d\tau)$ denote the space of square summable and absolutely summable functions over $\mathbb{A}$, respectively, that is,

$$\int_{\mathbb{A}} \left| f(s, \tau) \right|^2 \frac{ds}{s^2}\, d\tau < +\infty, \qquad \int_{\mathbb{A}} \left| f(s, \tau) \right| \frac{ds}{s^2}\, d\tau < +\infty, \tag{44}$$

where $s^{-2}\, ds\, d\tau$ is the left Haar measure of the affine group. The inner product of two functions $f_1$ and $f_2$ in $L^2(\mathbb{A}, s^{-2}\, ds\, d\tau)$ is defined as

$$\langle f_1, f_2 \rangle = \int_{\mathbb{A}} f_1(s, \tau) \overline{f_2(s, \tau)} \frac{ds}{s^2}\, d\tau. \tag{45}$$

The affine group is a nonunimodular group, where the right Haar measure is $s^{-1}\,ds\,d\tau$. Note that for the affine group, the modular function is given by $\Delta(s,\tau) = s^{-1}$.

## 2. *Fourier Transform over the Affine Group*

There are exactly two nonequivalent, infinite dimensional, irreducible, unitary representations of the affine group, that is, $\lambda \in \{+,-\}$ and $U((s,\tau),\pm) = U_{\pm}(s,\tau)$. Let $U_+$ act on the representation space $H_+$ that consists of functions $\varphi_+$, whose Fourier transforms are supported on the right half-line and $U_-$ act on $H_-$, the orthogonal complement of $H_+$, that consists of functions $\varphi_-$ whose Fourier transforms are supported on the left half-line. Note that $L^2(\mathbb{R}, dt)$ is a direct sum of $H_+$ and $H_-$, that is, $L^2(\mathbb{R}) = H_+ \oplus H_-$. Then, the representations

$$U_{\pm}(s,\tau)\varphi_{\pm}(t) = \frac{1}{\sqrt{s}}\varphi_{\pm}\left(\frac{t-\tau}{s}\right) \tag{46}$$

are unitary, nonequivalent, and irreducible in the space $H_+$ and $H_-$, respectively.

The affine Fourier transform of a function $f \in L^2(\mathbb{A}, s^{-2}\,ds\,d\tau)$ is defined as

$$\mathcal{F}_{\pm}(f) = \int_{-\infty}^{\infty}\int_{0}^{\infty} s^{-2}\,ds\,d\tau f(s,\tau)U_{\pm}(s,\tau). \tag{47}$$

The inverse affine Fourier transform is given by

$$f(s,\tau) = \sum_{\pm} \operatorname{trace}\big(U_{\pm}^{\dagger}(s,\tau)\mathcal{F}_{\pm}(f)\xi_{\pm}\big), \tag{48}$$

where $U_{\pm}^{\dagger}(s,\tau)$ denote the adjoint of $U_{\pm}(s,\tau)$ and $\xi_{\pm}$ are the Hermitian positive definite operators introduced in Eq. (12) for the affine group. They are defined as

$$\xi_{\pm}\varphi_{\pm}(t) = \mp\frac{\mathrm{i}}{2\pi}\frac{d\varphi_{\pm}}{dt}(t). \tag{49}$$

The convolution of two functions $f_1, f_2$ over the affine group is given by

$$(f_1 * f_2)(s,\tau) = \int_{-\infty}^{\infty}\int_{0}^{\infty} f_1(a,b) f_2\left(\frac{s}{a}, \frac{\tau-b}{a}\right)\frac{da}{a^2}\,db, \quad (s,\tau)\in\mathbb{A}. \tag{50}$$

Under the affine group Fourier transform, the convolution of two functions over the affine group becomes operator composition. More specifically,

$$\mathcal{F}_{\pm}(f_1 * f_2) = \mathcal{F}_{\pm}(f_1)\mathcal{F}_{\pm}(f_2). \tag{51}$$

Let $\{s^n_{\pm}(t)\}$ denote a set of orthonormal differentiable bases for $H_{\pm}$, respectively. Define $s^n(t) = s^n_+(t) + s^n_-(t)$, $U(s,\tau) = U_+(s,\tau) \oplus U_-(s,\tau)$, $(s,\tau) \in \mathbb{A}$, and $\xi = \xi_+ \oplus \xi_-$. Then for any $p \in L^2(\mathbb{R}, dx)$,

$$U(s,\tau)p = U_+(s,\tau)p_+ + U_-(s,\tau)p_- \tag{52}$$

and if $p$ is differentiable,

$$\xi p = \xi_+ p_+ + \xi_- p_-, \tag{53}$$

where $p_+$ and $p_-$ are orthogonal components of $p$ in $H_+$ and $H_-$, respectively.

For a given orthonormal, differentiable basis $\{s^n_{\pm}(t)\}$ of $H_{\pm}$, the inverse affine Fourier transform can be expressed as

$$\begin{aligned} f(s,\tau) &= \sum_{\pm}\sum_{n}\left\langle U^{\dagger}_{\pm}(s,\tau)\mathcal{F}_{\pm}(f)\xi_{\pm}s^n_{\pm}, s^n_{\pm}\right\rangle \\ &= \sum_{n}\left\langle \mathcal{F}(f)\xi s^n, U(s,\tau)s^n\right\rangle, \end{aligned} \tag{54}$$

where $\mathcal{F}(f) = \mathcal{F}_+(f) \oplus \mathcal{F}_-(f)$.

### B. *Target Reflectivity Estimation*

Observe that the echo model [Eq. (38)] is, in fact, the affine Fourier transform of the target reflectivity density function $T_W$ evaluated at the transmitted signal $p$;

$$e_T(t) = \mathcal{F}(T_W)p(t), \tag{55}$$

where $e_T$ is the received target echo. Now, assume that the unknown target reflectivity density function, $T_W(a,b)$, is a left affine stationary process contaminated with additive left affine stationary clutter $C(a,b)$ on the range-Doppler plane. It follows from Eqs. (29) and (31) that the optimal estimation for the target reflectivity density function in the mean square error sense is given by

$$\widetilde{T}_W = (T_W + C) * W_{\text{opt}}. \tag{56}$$

Here, $W_{\text{opt}}$ is the Wiener filter over the affine group given by

$$\mathcal{F}_{\pm}(W_{\text{opt}}) = \left(S^T_{\pm} + S^C_{\pm}\right)^{-1} S^T_{\pm}, \tag{57}$$

where $S_{\pm}^{T}$ and $S_{\pm}^{C}$ are the spectral density operators of the target and clutter, respectively.

The affine Wiener filter can be estimated from a priori target and clutter information. Such information is routinely compiled for air defense radar (see Nathanson *et al.*, 1999). The affine spectra, $S^T$ and $S^C$, of the target and clutter can be estimated from such information.

Alternatively, Eq. (56) can be expressed as

$$\mathcal{F}_{\pm}(\widetilde{T}_W) = \mathcal{F}_{\pm}(T_W + C)\mathcal{F}_{\pm}(W_{\text{opt}}) \tag{58}$$

or

$$\widetilde{T}_W(s, \tau) = \sum_{\pm} \operatorname{trace}\bigl(U_{\pm}^{\dagger}(s, \tau)\mathcal{F}_{\pm}(T_W + C)\mathcal{F}_{\pm}(W_{\text{opt}})\xi\bigr). \tag{59}$$

This estimate can be implemented in various forms leading to different adaptive receive and transmit algorithms (Yazici and Xie, 2005). Note that both target and clutter spectra, $S_{\pm}^{T}$ and $S_{\pm}^{C}$, are not Hermitian operators due to the nonunimodular nature of the affine group. However, it can be shown that $S_{\pm}^{T}\xi$ and $S_{\pm}^{C}\xi$ are Hermitian and nonnegative definite. So, we define

$$\widetilde{S}_{\pm}^{T} = S_{\pm}^{T}\xi \quad \text{and} \quad \widetilde{S}_{\pm}^{C} = S_{\pm}^{C}\xi. \tag{60}$$

Then, Eq. (59) can be rewritten as

$$\widetilde{T}_W(s, \tau) = \sum_{\pm} \operatorname{trace}\bigl(U_{\pm}^{\dagger}(s, \tau)\mathcal{F}_{\pm}(T_W + C)\xi\bigl(\widetilde{S}_{\pm}^{T} + \widetilde{S}_{\pm}^{C}\bigr)^{-1}\widetilde{S}_{\pm}^{T}\bigr). \tag{61}$$

Below, we describe an algorithm to implement the estimate given in Eq. (61) and discuss how the estimation problem couples with the waveform design problem.

### 1. *Receiver Design*

Let $\{s_{\pm}^{n}(t)\}$ be a set of orthonormal basis for $H_{\pm}$, respectively. Then, the target reflectivity estimate in Eq. (61) can be expressed as

$$\begin{aligned}\widetilde{T}_W(s, \tau) &= \sum_{\pm}\sum_{n}\bigl\langle\mathcal{F}_{\pm}(T_W + C)\xi\bigl(\widetilde{S}_{\pm}^{T} + \widetilde{S}_{\pm}^{C}\bigr)^{-1}\widetilde{S}_{\pm}^{T}s_{\pm}^{n}, U_{\pm}(s, \tau)s_{\pm}^{n}\bigr\rangle \\ &= \sum_{\pm}\sum_{n}\bigl\langle\mathcal{F}_{\pm}(T_W + C)\tilde{s}_{\pm}^{n}, U_{\pm}(s, \tau)s_{\pm}^{n}\bigr\rangle,\end{aligned} \tag{62}$$

where

$$\tilde{s}_{\pm}^{n} = \xi\bigl(\widetilde{S}_{\pm}^{T} + \widetilde{S}_{\pm}^{C}\bigr)^{-1}\widetilde{S}_{\pm}^{T}s_{\pm}^{n}. \tag{63}$$

Note that if $\tilde{s}^n = \tilde{s}^n_+ + \tilde{s}^n_-$ is chosen as the transmitted pulse, then $y^n(t) = \mathcal{F}(T_W + C)\tilde{s}^n$ becomes the received echo, and Eq. (62) can be reexpressed as

$$\widetilde{T}_W(s,\tau) = \sum_n \langle y^n, U(s,\tau)s^n \rangle. \tag{64}$$

This observation leads to the following algorithm for receiver and waveform design.

***Algorithm.***

1. Choose a set of orthonormal basis functions $\{s^n_\pm\}$ for $H_\pm$.
2. Transmit pulse $\tilde{s}^n = \tilde{s}^n_+ + \tilde{s}^n_-$, where $\tilde{s}^n_\pm = \xi(\widetilde{S}^T_\pm + \widetilde{S}^C_\pm)^{-1}\widetilde{S}^T_\pm s^n_\pm$.
3. At the receiver side, perform affine match filtering for each channel as follows:

$$z^n(s,\tau) = \langle y^n, U(s,\tau)s^n \rangle, \tag{65}$$

   where $y^n$ is the received echo for the $n$th channel.
4. Coherently sum all channels

$$\widetilde{T}_W(s,\tau) = \sum_n z^n(s,\tau). \tag{66}$$

So far, we have not specified how we can choose the set of orthonormal basis functions $\{s^n_\pm\}$. Therefore, the wideband image formation algorithms described above are valid independent of the choice of transmitted waveforms. The orthogonal functions $\{s^n_\pm\}$ or their filtered counterparts $\{\tilde{s}^n_\pm\}$ do not need to be wideband signals. Thus, this reconstruction formula leads to a scenario where there are multiple radars/sonars operating independently, each with a limited low-resolution aperture (i.e., narrowband transmission). Nevertheless, appropriate processing and fusion of data from multiple narrowband sensors lead to formation of a synthetic wideband image.

### *C. Waveform Design*

Note that in the image reconstruction described above, the MMSE is achieved irrespective of the basis functions or the transmitted pulses chosen. However, the requirement is that a complete set of modified basis functions $\{\tilde{s}^n\}$ must be transmitted to achieve the MMSE. In reality, we are only allowed to transmit finite number of, for instance $N$, waveforms. So the question is how to choose the $N$ best waveforms to achieve MMSE sense.

Observe that the MMSE estimate in Eq. (59) can be written as

$$\widetilde{T}_W(s,\tau) = \sum_{\pm} \operatorname{trace}\big(U_{\pm}^{\dagger}(s,\tau)\mathcal{F}_{\pm}(\widetilde{T}_W)\xi\big) \tag{67}$$

$$= \sum_{\pm}\sum_{n}\big\langle \mathcal{F}_{\pm}(\widetilde{T}_W)\xi s_{\pm}^{n}, U_{\pm}(s,\tau)s_{\pm}^{n}\big\rangle, \tag{68}$$

where $\{s_{\pm}^{n}\}$ are orthonormal bases for $H_{\pm}$, $s_{\pm}^{n} = s_{+}^{n} + s_{-}^{n}$.

Let $T_n(s,\tau) = \langle \mathcal{F}(\widetilde{T}_W)\xi s^n, U(s,\tau)s^n\rangle$. Then,

$$\widetilde{T}_W(s,\tau) = \sum_{n} T_n(s,\tau). \tag{69}$$

It can be easily verified that $\widetilde{T}_W(s,\tau)$ and $T_n(s,\tau)$ are affine stationary processes with the following properties:

1. $T_n(s,\tau)$ and $T_m(s,\tau)$ are jointly affine stationary.
2. $E[T_n(s,\tau)\overline{T_m(s,\tau)}] = 0$ if $n \neq m$.
3. $E[T_n(s,\tau)\overline{\widetilde{T}_W(s,\tau)}] = E[|T_n(s,\tau)|^2] = \langle \mathcal{F}(R_{\widetilde{T}_W})\xi s^n, s^n\rangle$, where $R_{\widetilde{T}_W}$ is the autocorrelation function of $\widetilde{T}_W(s,\tau)$.
4. $E[|\widetilde{T}_W(s,\tau)|^2] = \sum_{\pm} \operatorname{trace}(\mathcal{F}_{\pm}(R_{\widetilde{T}_W})\xi)$.
5. $R_{\widetilde{T}_W} = W_{\text{opt}}^{*} * (R_T + R_C) * W_{\text{opt}}$, where $W_{\text{opt}}^{*}(s,\tau) = \overline{W_{\text{opt}}((s,\tau)^{-1})}$ and $R_T$, $R_C$ are autocorrelation functions of target reflectivity density process $T(s,\tau)$ and clutter $C(s,\tau)$, respectively.

It follows from the above properties that if only $N$ pulses are transmitted, then the mean square error is given by

$$\begin{aligned}
E\left[\left|\widetilde{T}_W - \sum_{n=1}^{N} T_n\right|^2\right] &= E\big[|\widetilde{T}_W|^2\big] + \sum_{n=1}^{N} E\big[|T_n|^2\big] - 2\sum_{n=1}^{N} E[T_n\overline{\widetilde{T}_W}] \\
&= \sum_{\pm} \operatorname{trace}\big(\mathcal{F}_{\pm}(R_{\widetilde{T}_W})\xi\big) - \sum_{n=1}^{N}\big\langle \mathcal{F}_{\pi}(R_{\widetilde{T}_W})\xi s^n, s^n\big\rangle \\
&= \sum_{\pm} \operatorname{trace}\big(\mathcal{F}_{\pm}(R_{\widetilde{T}_W})\xi\big) - \sum_{\pm}\sum_{n=1}^{N}\big\langle \mathcal{F}_{\pm}(R_{\widetilde{T}_W})\xi s_{\pm}^n, s_{\pm}^n\big\rangle \\
&= \sum_{\pm}\sum_{n=N+1}^{\infty}\big\langle \mathcal{F}_{\pm}(R_{\widetilde{T}_W})\xi s_{\pm}^n, s_{\pm}^n\big\rangle.
\end{aligned} \tag{70}$$

Note that

$$\begin{aligned}\mathcal{F}_{\pm}(R_{\widetilde{T}_W})\xi &= \mathcal{F}_{\pm}\big(W_{\mathrm{opt}}^{*} * (R_T + R_N) * W_{\mathrm{opt}}\big)\xi \\ &= \mathcal{F}_{\pm}(W_{\mathrm{opt}}^{*})\big(S_{\pm}^{T} + S_{\pm}^{N}\big)\big(S_{\pm}^{T} + S_{\pm}^{N}\big)^{-1} S_{\pm}^{T}\xi \\ &= \mathcal{F}_{\pm}(W_{\mathrm{opt}}^{*})\widetilde{S}_{\pm}^{T}. \end{aligned} \tag{71}$$

Therefore, the MMSE is achieved if $s_{\pm}^{n}$, $n = 1, \ldots, N$, are chosen as the eigenfunctions of the operators $\mathcal{F}_{\pm}(W_{\mathrm{opt}}^{*})\widetilde{S}_{\pm}^{T}$ corresponding to the $N$ largest eigenvalues. Thus, step 1 of the algorithm introduced in the previous subsection can be modified so that the orthonormal functions $\{s_{\pm}^{n}\}$, $n = 1, \ldots, N$, are chosen as the unit eigenfunctions of $\mathcal{F}_{\pm}(W_{\mathrm{opt}}^{*})\widetilde{S}_{\pm}^{T}$ corresponding to $N$ largest eigenvalues.

### *D. Numerical Experiments*

For ease of computation, transmitted waveforms used in the numerical simulations are derived from the Laguerre polynomials.

Let

$$\hat{s}_{+}^{n}(\omega) = L_{n-1}(\omega)\mathrm{e}^{-\omega/2}, \quad \omega \in \mathbb{R}^{+}, n \in \mathbb{N}, \tag{72}$$

where $\hat{s}_{+}^{n}(\omega)$ is the Fourier transform of $s_{+}^{n}(t)$ and $L_{n-1}$, $n \in \mathbb{N}$, are Laguerre polynomials defined by

$$L_0(x) = 1, \tag{73}$$

$$L_1(x) = -x + 1, \tag{74}$$

$$L_{n+1}(x) = \frac{2n + 1 - x}{n + 1} L_n(x) - \frac{n}{n + 1} L_{n-1}(x), \quad n \in \mathbb{N}. \tag{75}$$

It is well known that (Abramowitz and Stegun, 1972)

$$\int_0^\infty \mathrm{e}^{-x} L_m(x) L_n(x)\, dx = \begin{cases} 1 & m = n, \\ 0 & \text{else}. \end{cases} \tag{76}$$

Therefore, $\{\hat{s}_{+}^{n}\}$ is an orthonormal basis for $L^2(\mathbb{R}^{+}, dx)$. Let $s_{+}^{n}$ be the standard inverse Fourier transform of $\hat{s}_{+}^{n}$. Then, $\{s_{+}^{n}\}$ is an orthonormal basis for $H_{+}$. Let $\hat{s}_{-}^{n}(\omega) = \hat{s}_{+}^{n}(-\omega)$, $\omega \in \mathbb{R}^{-}$. Then, $s_{-}^{n}(t) = \overline{s_{+}^{n}(t)}$, $t \in \mathbb{R}$, and $\{s_{-}^{n}\}$ are orthonormal bases for $H_{-}$.

We generated realizations of the target and clutter based on the following spectral density operators $\widetilde{S}_{\pm}^{T}$ and $\widetilde{S}_{\pm}^{C}$ with respect to bases $\{s_{\pm}^{n}\}$:

$$\widetilde{S}_{\pm}^{T} = \begin{pmatrix} 10 & 4.5 & & & & & & & & \\ 4.5 & 9 & 4 & & & & & & & \\ & 4 & 8 & 3.5 & & & & & & \\ & & 3.5 & 7 & 3 & & & & & \\ & & & 3 & 6 & 2.5 & & & & \\ & & & & 2.5 & 5 & 2 & & & \\ & & & & & 2 & 4 & 1.5 & & \\ & & & & & & 1.5 & 3 & 1 & \\ & & & & & & & 1 & 2 & 0.5 \\ & & & & & & & & 0.5 & 1 \end{pmatrix} \quad \text{and} \tag{77}$$

$$\widetilde{S}_{\pm}^{C} = \begin{pmatrix} 0_{7\times 7} & & & & & & \\ & 4 & & & & & \\ & & 8 & & & & \\ & & & 10 & & & \\ & & & & 12 & & \\ & & & & & \ddots & \\ & & & & & & 40 \end{pmatrix}.$$

Figures 2a and 2b show a realization of the target and target contaminated with clutter.

We synthesized 10 realizations of the target and clutter at various signal-to-clutter ratios (SCR) defined as $SCR = 20\log_{10}(\sigma_s^2/\sigma_c^2)$, where $\sigma_s^2$ and $\sigma_c^2$ are the target and clutter variance, respectively. Each realization is generated according to spectral densities $\sigma_s^2\widetilde{S}_{\pm}^{T}$ and $\sigma_c^2\widetilde{S}_{\pm}^{C}$. The transmitted waveforms are chosen as

$$\bar{s}^n = \xi\left(\widetilde{S}^T + \widetilde{S}^C\right)^{-1}\widetilde{S}^T s^n, \quad n = 1, \ldots, 20. \tag{78}$$

Figures 2c and 2d present results obtained using the algorithm in Section V.B and Naparst's (1991) method. For Naparst's method, transmitted pulses are the Hermite polynomial basis (Naparst, 1991). Figure 3 shows the mean square error (MSE) between the true and estimated reflectivity density functions for the proposed method and Naparst's method at different SCR levels. MSE is calculated by averaging error based on 10 realizations of the true target and the estimated target at each SCR level. Our numerical study shows that the proposed method yields lower MSE than Naparst's method, particularly for low SCR.

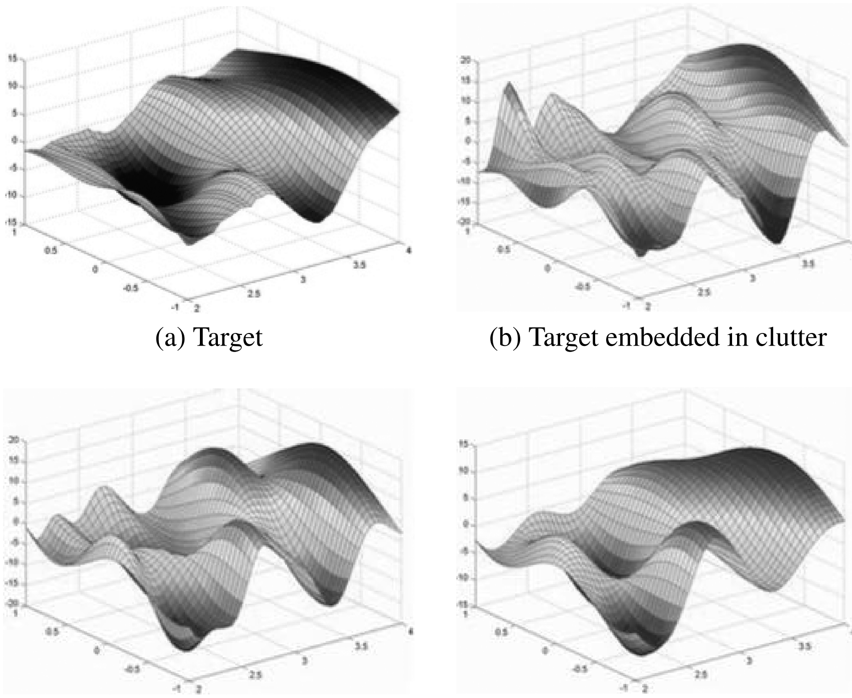

(a) Target (b) Target embedded in clutter

(c) Naparst's method (d) Proposed method

FIGURE 2. Estimated target reflectivity function embedded in clutter. (a) True target reflectivity function. (b) Target reflectivity function embedded in clutter. (c) Estimated target reflectivity function using Naparst's method. (d) Estimated target reflectivity function by the proposed method.

## VI. RADON AND EXPONENTIAL RADON TRANSFORMS

In transmission computed tomography, a X-ray beam with known energy is sent through an object, and attenuated X-rays are collected by an array of detectors. The attenuation in the final X-ray beam provides a means of determining the mass density of the object along the path of the X-ray. In two dimensions, the relationship between the attenuation and mass density along the X-ray path is given by the Radon transform. In general, the *Radon transform* $\mathcal{R}$ maps an integrable function $f$ (unknown image) over $\mathbb{R}^N$ to its integral over the hyperplanes of $\mathbb{R}^N$ (Radon, 1917; Deans, 1983; Natterer, 1986; Helgason, 1999)

$$(\mathcal{R}f)(\boldsymbol{\vartheta}, r) \int_{\mathbb{R}^N} f(\boldsymbol{x})\delta(\boldsymbol{x} \cdot \boldsymbol{\vartheta} - r)\, d\boldsymbol{x}, \tag{79}$$

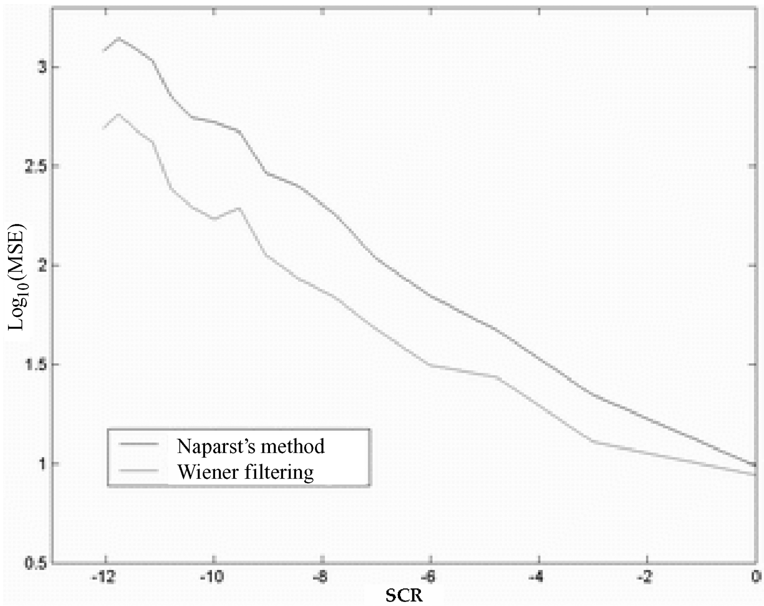


FIGURE 3. Mean square error between the estimated and true target reflectivity function.

where $\boldsymbol{\vartheta}$ is the unit normal of the hyperplane, which is an element of the unit sphere $S^{N-1}$ in $\mathbb{R}^N$, and $r \geq 0$ is the distance from the hyperplane to the origin. While for the current discussion we will take $N = 2$, the results are valid for any $N \in \mathbb{Z}$ greater than 2 (Yarman and Yazici, 2005c).

There has been an enormous interest in both applied and theoretical communities in analyzing and developing methods of inversion for the Radon transform (Barrett, 1984; Cormack, 1963, 1964; Gelfand *et al.*, 1966; Helgason, 1999; Natterer, 1986; Pintsov, 1989). Although the research effort has been very diverse, inversion of the Radon transform can be broadly categorized into two approaches: analytic and algebraic. The analytic approach covers the works of Cormack (1964), Natterer (1986), and Barrett (1984) among many others. The research effort in this approach ultimately aims at numerical implementation of the Radon transform inversion. The foremost study in the algebraic approach can be found in the work of Helgason (1999) and the references therein. The algebraic approach is mainly concerned with the generalization of the Radon transform and the development of associated analysis methods in a group theoretic setting (Helgason, 1999, 2000; Gelfand *et al.*, 1966; Rouviére, 2001; Strichartz, 1981). In Helgason (1999), the domain of the unknown function and its projections are given by the homogeneous spaces of the Euclidean motion group, $M(N)$, of the $N$-dimensional

Euclidean space, namely by $M(N)/SO(N)$ and $M(N)/(\mathbb{Z}^2 \times M(N-1))$. The underlying group structure enables development of a generalization of the Radon transform for the homogeneous spaces of locally compact unimodular groups. This leads to a generalization of the backprojection operator and the development of generalized filtered backprojection-type inversion methods for the generalized Radon transforms.

In emission tomography, an object is identified with the emission distribution of a radiochemical substance inside the object. The measurements depend on both the emission distribution of the radiochemical substance and the attenuation distribution of the object. For a uniform attenuation, the relationship between the measurements and the emission distribution is represented by the *exponential Radon transform*. The exponential Radon transform of a compactly supported real valued function $f$ over $\mathbb{R}^2$ for a uniform attenuation coefficient $\mu \in \mathbb{C}$, is defined as (Natterer, 1986)

$$(\mathcal{T}_\mu f)(\boldsymbol{\vartheta}, t) = \int_{\mathbb{R}^2} f(\boldsymbol{x})\delta(\boldsymbol{x} \cdot \boldsymbol{\vartheta} - t)\mathrm{e}^{\mu \boldsymbol{x} \cdot \boldsymbol{\vartheta}^\perp}\, d\boldsymbol{x}, \tag{80}$$

where $t \in \mathbb{R}$, $\boldsymbol{\vartheta} = (\cos\theta, \sin\theta)^T$ is a unit vector on $S^1$ with $\theta \in [0, 2\pi)$ and $\boldsymbol{\theta}^\perp = (-\sin\theta, \cos\theta)^T$. Clearly, Radon transform is a special case of the exponential Radon transform for which $\mu = 0$.

The exponential Radon transform constitutes a mathematical model for imaging modalities such as X-ray tomography ($\mu = 0$) (Cormack, 1963), single photon emission tomography (SPECT) ($\mu \in \mathbb{R}$) (Tretiak and Metz, 1980), and optical polarization tomography of stress tensor field ($\mu \in \mathrm{i}\mathbb{R}$) (Puro, 2001).

A number of different approaches have been proposed for the exponential Radon transform inversion (Bellini *et al.*, 1979; Tretiak and Metz, 1980; Inouye *et al.*, 1989; Hawkins *et al.*, 1988; Kuchment and Shneiberg, 1994; Metz and Pan, 1995). Bellini *et al.* (1979) reduced the inversion of the exponential Radon transform to finding the solution of an ordinary differential equation that leads to a relationship between the circular harmonic decomposition of the Fourier transform of the projections $(\mathcal{T}_\mu f)$ and circular harmonic decomposition of the Fourier transform of the function $f$. An alternative method based on the circular harmonic decomposition of the Fourier transform of $f$ and $(\mathcal{T}_\mu f)$ was derived by Tretiak and Metz (1980) and Inouye *et al.* (1989) using two different approaches.

Tretiak and Metz (1980) also introduced a filtered backprojection-type inversion method. Hawkins *et al.* (1988) used the filtered backprojection method introduced by Tretiak and Metz together with the circular harmonic decomposition and expressed the circular harmonic decomposition of the function $f$ in terms of the circular harmonic decomposition of its projections

$(\mathcal{T}_\mu f)$. Later the filtered backprojection method was extended to the angle-dependent exponential Radon transform by Kuchment and Shneiberg (1994).

Reconstruction of images from the data collected by the aforementioned imaging systems requires inversion of the exponential Radon transform.

Here we present an alternative deconvolution-type inversion approach for the Radon and exponential Radon transforms based on the harmonic analysis of the Euclidean motion group. The proposed deconvolution-type inversion method is a special case of the Wiener filtering method presented in Section IV. In the current discussion, we address the inversion problem in a deterministic setting. However, it should be noted that many emission tomography applications require rigorous treatment of noise, which can be addressed by extending the approach presented here to the statistical setting introduced in Section IV. Furthermore, the inversion algorithm can be implemented efficiently using the fast Fourier algorithms over $M(2)$ (Kyatkin and Chirikjian, 2000; Yarman and Yazici, 2003, 2005a, 2005b, 2005c, 2005d).

### *A. Fourier Transform over $M(2)$*

The rigid motions of $\mathbb{R}^2$ form a group called the Euclidean motion group $M(2)$. The elements of the group are the $3 \times 3$ dimensional matrices of the form

$$(R_\theta, \boldsymbol{r}) = \begin{bmatrix} R_\theta & \boldsymbol{r} \\ \boldsymbol{0}^T & 1 \end{bmatrix}, \quad R_\theta \in SO(2),\ \boldsymbol{r} \in \mathbb{R}^2, \tag{81}$$

parameterized by a rotation component $\theta$ and a translation component $\boldsymbol{r}$. $SO(2)$ is the special orthonormal group, whose elements are $2\times 2$-dimensional matrices with determinant equal to 1, and the group operation is the usual matrix multiplication. The group operation of $M(2)$ is the usual matrix multiplications, and the inverse of an element is obtained by matrix inversion as $(R_\theta, \boldsymbol{r})^{-1} = (R_\theta^{-1}, -R_\theta^{-1}\boldsymbol{r})$.

Let $f_1$ and $f_2$ be two integrable functions over $M(2)$. Then, the inner product $\langle f_1, f_2\rangle$ and convolution $(f_1 * f_2)$ of $f_1$ and $f_2$ are defined as

$$\langle f_1, f_2\rangle = \int_{M(2)} f_1(R_\phi, \boldsymbol{x})\overline{f_2(R_\phi, \boldsymbol{x})}\, d(R_\phi)\, d\boldsymbol{x}, \tag{82}$$

$$(f_1 * f_2)(R_\theta, \boldsymbol{r}) = \int_{M(2)} f_1(R_\theta R_\phi, R_\theta \boldsymbol{x} + \boldsymbol{r}) f_2\big(R_\phi^{-1}, -R_\phi^{-1}\boldsymbol{x}\big)\, d(R_\phi)\, d\boldsymbol{x}, \tag{83}$$

where $(R_\theta, \boldsymbol{r}), (R_\phi, \boldsymbol{x}) \in M(2)$, and $d(R_\phi)\, d\boldsymbol{x}$ is the normalized invariant Haar measure on $M(2)$, with $d(R_\phi)$ being the normalized measures on $SO(2)$.

For an explanation of $\int_{SO(2)} d(R_\phi)$, we refer the reader to Section VII.2 of Natterer (1986).

Let $f$ be a function defined over $M(2)$. $f$ is said to be $L^2(M(2), d(R_\phi)\,d\boldsymbol{x})$ if

$$\int_{M(2)} \left|f(R_\phi, \boldsymbol{x})\right|^2 d(R_\phi)\; d\boldsymbol{x} < \infty. \tag{84}$$

The irreducible unitary representations $U((R_\theta, \boldsymbol{r}), \lambda)$ of $M(2)$ are given by the following linear operators (Vilenkin, 1988)

$$\big(U\big((R_\theta, \boldsymbol{r}), \lambda\big)F\big)(\boldsymbol{s}) = \mathrm{e}^{-\mathrm{i}\lambda(\boldsymbol{r}\cdot\boldsymbol{s})} F\big(R_\theta^{-1}\boldsymbol{s}\big), \quad F \in L^2\big(S^1, d(\boldsymbol{\omega})\big), \tag{85}$$

where $\boldsymbol{s}$ is a point on the unit circle $S^1$, $(\,\cdot\,)$ is the standard inner product over $\mathbb{R}^2$, and $\lambda$ is a nonnegative real number.

Since the *circular harmonics* $\{S_m\}$ form an orthonormal basis for $L^2(S^1, d(\boldsymbol{\omega}))$ (Seeley, 1966), the matrix elements $U_{mn}((R_\theta, \boldsymbol{r}), \lambda)$ of $U((R_\theta, \boldsymbol{r}), \lambda)$ are given by Vilenkin (1988):

$$\begin{aligned} U_{mn}\big((R_\theta, \boldsymbol{r}), \lambda\big) &= \big(S_m, U\big((R_\theta, \boldsymbol{r}), \lambda\big)S_n\big) \\ &= \int_{S^1} \overline{S_m(\boldsymbol{\omega})}\mathrm{e}^{-\mathrm{i}\lambda\boldsymbol{r}\cdot\boldsymbol{\omega}} S_n\big(R_\theta^{-1}\boldsymbol{\omega}\big)\, d(\boldsymbol{\omega}), \end{aligned} \tag{86}$$

where $d(\boldsymbol{\omega})$ is the normalized Haar measure on the unit circle.

If the complex exponentials $\{\mathrm{e}^{in\psi}\}$, $n \in \mathbb{Z}$ are chosen as the orthonormal basis for $L^2(S^1, d(\boldsymbol{\omega}))$, the matrix elements for the unitary representation $U(g, \lambda)$ of $M(2)$ become (Vilenkin, 1988)

$$\begin{aligned} &U_{mn}\big((R_\theta, \boldsymbol{r}), \lambda\big) \\ &\quad = \big(\mathrm{e}^{\mathrm{i}m\psi}, U\big((R_\theta, \boldsymbol{r}), \lambda\big)\mathrm{e}^{\mathrm{i}n\psi}\big) \\ &\quad = \frac{1}{2\pi}\int_0^{2\pi} \mathrm{e}^{-\mathrm{i}m\psi}\mathrm{e}^{-\mathrm{i}(r_1\lambda\cos\psi + r_2\lambda\sin\psi)}\mathrm{e}^{\mathrm{i}n(\psi-\theta)}\, d\psi, \quad \forall m, n \in \mathbb{Z}. \end{aligned} \tag{87}$$

The matrix elements of $U((R_\theta, \boldsymbol{r}), \lambda)$ satisfy the following properties:

$$U_{mn}\big(\big(R_\theta^{-1}, -R_\theta^{-1}\boldsymbol{r}\big), \lambda\big) = U_{mn}^{-1}\big((R_\theta, \boldsymbol{r}), \lambda\big) = \overline{U_{nm}(g, \lambda)}, \tag{88}$$

$$U_{mn}\big((R_\phi R_\theta, R_\phi\boldsymbol{r} + \boldsymbol{x}), \lambda\big) = \sum_k U_{mk}\big((R_\phi, \boldsymbol{x}), \lambda\big)U_{kn}\big((R_\theta, \boldsymbol{r}), \lambda\big). \tag{89}$$

Furthermore, the matrix elements $U_{mn}((R_\theta, \boldsymbol{r}), \lambda)$ of $U((R_\theta, \boldsymbol{r}), \lambda)$ form a complete orthonormal system in $L^2(M(2), d(R_\phi)\,d\boldsymbol{x})$.

Let $f \in L^2(M(2))$. The *Fourier transform over* $M(2)$ of $f$ is defined as (Sugiura, 1975; Vilenkin, 1988)

$$\mathcal{F}(f)(\lambda) = \hat{f}(\lambda) = \int_{M(2)} f(R_\theta, \boldsymbol{r}) U\big((R_\theta, \boldsymbol{r})^{-1}, \lambda\big)\, d(R_\theta)\, d\boldsymbol{r}, \qquad (90)$$

where $d(R_\theta)\, d\boldsymbol{r} = d\boldsymbol{r} d(R_\theta)$ is the normalized Haar measure on $M(2)$. Then, the *inverse Fourier transform* is given by

$$\begin{aligned}\mathcal{F}^{-1}(\hat{f})(R_\theta, \boldsymbol{r}) &= f(R_\theta, \boldsymbol{r}) \\ &= \frac{1}{(2\pi)^2} \int_0^\infty \operatorname{trace}\big(\hat{f}(\lambda) U\big((R_\theta, \boldsymbol{r}), \lambda\big)\big) \lambda\, d\lambda. \end{aligned} \qquad (91)$$

The matrix elements of the Fourier transform over $M(2)$ is given by

$$\mathcal{F}(f)_{mn}(\lambda) = \hat{f}_{mn}(\lambda) = \int_{M(2)} f(R_\theta, \boldsymbol{r}) U_{mn}\big((R_\theta, \boldsymbol{r})^{-1}, \lambda\big)\, d(R_\theta)\, d\boldsymbol{r}, \qquad (92)$$

for $\lambda > 0$. Then the corresponding *inverse Fourier transform* is given by

$$\begin{aligned}\mathcal{F}^{-1}(\hat{f}_{mn})(R_\theta, \boldsymbol{r}) &= f(R_\theta, \boldsymbol{r}) \\ &= \frac{1}{(2\pi)^2} \int_0^\infty \sum_{m,n} \hat{f}_{mn}(\lambda) U_{nm}\big((R_\theta, \boldsymbol{r}), \lambda\big) \lambda\, d\lambda. \end{aligned} \qquad (93)$$

Let $f,\ f_1,\ f_2 \in L^2(M(2), d(R_\phi)\, d(\boldsymbol{x}))$. The Fourier transform over $M(2)$ satisfies the following properties:

1. *Adjoint property*:

$$\widehat{f^*}_{mn}(\lambda) = \overline{\hat{f}_{nm}(\lambda)}, \qquad (94)$$

   where $f^*(R_\theta, \boldsymbol{r}) = \overline{f((R_\theta, \boldsymbol{r})^{-1})}$.
2. *Convolution property*:

$$\mathcal{F}(f_1 * f_2)_{mn}(\lambda) = \sum_q \widehat{f_2}_{mq}(\lambda) \widehat{f_1}_{qn}(\lambda). \qquad (95)$$

3. *Plancherel relation*: Let

$$\langle \widehat{f_1}, \widehat{f_2} \rangle = \frac{1}{(2\pi)^2} \int_0^\infty \sum_{m,n} \widehat{f_1}_{mn}(\lambda) \widehat{f_2^*}_{nm}(\lambda) \lambda\, d\lambda, \qquad (96)$$

   then $\langle f_1, f_2 \rangle = \langle \widehat{f_1}, \widehat{f_2} \rangle$.

4. *SO*(2) *invariance—I*: If $f$ is a $SO(2)$ invariant function over $M(2)$, that is, $f(g) = f(\boldsymbol{r}) \in L^2(\mathbb{R}^2)$, then

$$\hat{f}_{mn}(\lambda) = \delta_m \tilde{f}_n(-\lambda), \tag{97}$$

where $\delta_m$ is the Kronecker delta function, and $\tilde{f}_n(\lambda)$ is the spherical harmonic decomposition of the standard Fourier transform $\tilde{f}$ of $f$

$$\tilde{f}_n(\lambda) = \int_{S^1} \tilde{f}(\lambda\boldsymbol{\omega}) S_m(\boldsymbol{\omega})\, d(\boldsymbol{\omega}), \quad \text{where } \tilde{f}(\boldsymbol{\varepsilon}) = \int_{\mathbb{R}^2} f(\boldsymbol{x}) \mathrm{e}^{-\mathrm{i}\boldsymbol{\varepsilon}\cdot\boldsymbol{x}}\, d\boldsymbol{x}. \tag{98}$$

5. *SO*(2) *invariance—II*: Let $f$ be a $SO(2)$ invariant function over $M(2)$ and $\varphi(g) = \delta(R_\theta) f(\boldsymbol{r})$, then

$$\widehat{\varphi}_{mn}(\lambda) = \int_{S^1} \tilde{f}(-\lambda\boldsymbol{\omega}) S_n(\boldsymbol{\omega}) \overline{S_m(\boldsymbol{\omega})}\, d(\boldsymbol{\omega}), \tag{99}$$

and $\widehat{\varphi}_{0n}(\lambda) = \tilde{f}_n(-\lambda)$.

The Fourier transform over $M(2)$ can be extended to the space of compactly supported functions $\mathcal{D}(M(2))$ and rapidly decreasing functions $\mathcal{S}(M(2))$ and is injective (Sugiura, 1975). Furthermore, Fourier transform over $M(2)$ can be extended to the space of tempered distributions $\mathcal{S}'(M(2))$ and compactly supported distributions $\mathcal{E}'(M(2))$, together with its properties as shown in Appendix B.

### B. *Radon and Exponential Radon Transforms as Convolutions*

#### 1. *Radon Transform*

Let $\delta(R_\phi)$ denote the distribution over $SO(2)$ defined as follows:

$$\int_{SO(2)} \delta(R_\phi)\varphi(R_\phi)\, d(R_\phi) = \varphi(I), \tag{100}$$

where $I$ is the identity rotation. Let $g = (R_\theta, \boldsymbol{r})$, $h = (R_\phi, \boldsymbol{x}) \in M(2)$, $\boldsymbol{\vartheta} = R_\theta^T \boldsymbol{e_1}$, and $r_1 = \boldsymbol{r} \cdot \boldsymbol{e_1}$, where $\boldsymbol{e_i}$ denotes the unit vector in $\mathbb{R}^2$ with its $i$th component equal to 1. Then, the Radon transform of a real valued function $f$ can be written as a convolution over $M(2)$ as follows:

$$
\begin{aligned}
(\mathcal{R}f)(\boldsymbol{\vartheta}, -r_1) &= \int_{\mathbb{R}^2} f(\boldsymbol{x})\delta\big(\boldsymbol{x}\cdot R_\theta^T\boldsymbol{e_1} + r_1\big)\,d\boldsymbol{x} \\
&= \int_{SO(2)}\int_{\mathbb{R}^2} \delta\big((R_\theta\boldsymbol{x} + r)\cdot\boldsymbol{e_1}\big)\delta(R_\phi)f(\boldsymbol{x})\,d\boldsymbol{x}\,d(R_\phi) \\
&= \int_{M(2)} \Lambda_{\mathcal{R}}(gh)f'(h)\,d(R_\phi)\,d\boldsymbol{x} \\
&= (\Lambda_{\mathcal{R}} * f'^{*})(g),
\end{aligned}
\tag{101}
$$

where $f^*(h) = \overline{f(h^{-1})}$, $\Lambda_{\mathcal{R}}(h) = \delta(\boldsymbol{x}\cdot\boldsymbol{e_1})$, $\delta$ being the Dirac delta distribution (Gelfand and Shilov, 1964), and $f'(h) = \delta(R_\phi)f(\boldsymbol{x})$. Alternative formulations of the convolution representation of the Radon transform were given in Yarman and Yazici (2003, 2005c, 2005d). Note that for the rest of this chapter, we shall use the integral representation of distributions.

2. *Exponential and Angle-Dependent Exponential Radon Transforms*

Motivated by the Radon transform, we now present the convolution representations of the angle-dependent exponential Radon transform.

Let $\boldsymbol{\vartheta} = R_\theta^T\boldsymbol{e_1}$, and $r_1 = \boldsymbol{r}\cdot\boldsymbol{e_1}$, for some $R_\theta \in SO(2)$. The *angle-dependent exponential Radon* transform of a real valued function is given by

$$
\begin{aligned}
(\mathcal{T}_{\mu(\boldsymbol{\vartheta})}f)(\boldsymbol{\vartheta}, -r_1) &= \int_{\mathbb{R}^2} f(\boldsymbol{x})\delta(\boldsymbol{x}\cdot\boldsymbol{\vartheta} + r_1)\mathrm{e}^{\mu(\boldsymbol{\vartheta})\boldsymbol{x}\cdot\boldsymbol{\vartheta}^\perp}\,d\boldsymbol{x} \\
&= \int_{SO(2)}\int_{\mathbb{R}^2} f(\boldsymbol{x})\delta(R_\phi)\delta\big((R_\theta\boldsymbol{x} + \boldsymbol{r})\cdot\boldsymbol{e_1}\big) \\
&\quad\times \exp\big(\mu\big((R_\theta R_\phi)^T\boldsymbol{e_2}\big)R_\theta\boldsymbol{x}\cdot\boldsymbol{e_2}\big)\,d\boldsymbol{x}\,d(R_\phi).
\end{aligned}
\tag{102}
$$

Multiplying both sides of (102) by $\mathrm{e}^{\mu(\boldsymbol{\vartheta})r_2}$, the resulting operator $(\mathcal{T}'_{\mu(\boldsymbol{\vartheta})}f)$ can be represented as a convolution over $M(2)$

$$
\begin{aligned}
(\mathcal{T}'_{\mu(\boldsymbol{\vartheta})}f)(g) &= \mathrm{e}^{\mu(\boldsymbol{\vartheta})r_1}(\mathcal{T}_{\mu(\boldsymbol{\vartheta})}f)(\boldsymbol{\vartheta}, \boldsymbol{y}) \\
&= (\Lambda_{\mathcal{T}'_\mu(\boldsymbol{\theta})} * f'^{*})(g),
\end{aligned}
\tag{103}
$$

where $f'(g) = \delta(R_\theta)f(\boldsymbol{r})$ and $\Lambda_{\mathcal{T}'_\mu(\boldsymbol{\vartheta})}(g) = \delta(\boldsymbol{r}\cdot\boldsymbol{e_1})\mathrm{e}^{\mu(\boldsymbol{R_\theta^T e_2})\boldsymbol{r}\cdot\boldsymbol{e_2}}$.

From Eq. (103) the angle-dependent exponential Radon transform can be visualized as an operator that fixes the function $f$ while traversing an exponentially weighted projection line, where the weight is determined by the orientation of the line. When $\mu$ is independent of the angle, that is, $\mu(\boldsymbol{\vartheta}) = \mu$

for some fixed $\mu \in \mathbb{C}$, the angle-dependent exponential Radon transform reduces to the exponential Radon transform

$$(\mathcal{T}'_\mu f)(g) = \mathrm{e}^{\mu r_2}(\mathcal{T}_\mu f)(\boldsymbol{\vartheta}, -r_1).$$

We refer to $(\mathcal{T}'_\mu f)$ as the modified exponential Radon transform of $f$.

### *C. Inversion Methods*

Let $\mathcal{A} \in \{\mathcal{R}, \mathcal{T}'_\mu\}$. Then, one can treat $(\mathcal{A}f)$ as a tempered distribution that is the convolution of two distributions (see Appendix B for the definition of convolution of distributions), $\Lambda_A$, and $f'$ given as in Section VI.B

$$(\mathcal{A}f)(g) = (\Lambda_\mathcal{A} * f'^{*})(g), \tag{104}$$

in which $f'$ is compactly supported and $\Lambda_\mathcal{A} \in \mathcal{S}'(M(2))$.

Using the convolution property of the Fourier transform over $M(2)$, Eq. (104) can be written as (see Appendix B for Fourier transform of distributions over $M(2)$)

$$\widehat{(\mathcal{A}f)}(\lambda) = \hat{f'}^{\dagger}(\lambda)\widehat{\Lambda_\mathcal{A}}(\lambda). \tag{105}$$

If $\widehat{\Lambda_\mathcal{A}}(\lambda)$ is invertible, then $f'$ can be obtained as

$$f'(h) = \mathcal{F}^{-1}\big(\big[\widehat{(\mathcal{A}f)}(\lambda)\big[\widehat{\Lambda_\mathcal{A}}(\lambda)\big]^{-1}\big]^{\dagger}\big). \tag{106}$$

Since $\widehat{\Lambda_\mathcal{A}}(\lambda)$ is rank deficient, we replace the inverse of $\widehat{\Lambda_\mathcal{A}}(\lambda)$ with the special case of the optimal filter $\widehat{W}_{\mathrm{opt}}(\lambda)$ Eq. (35) of Section IV, given as

$$\widehat{W}_{\mathrm{opt}}(\lambda) = \big[\widehat{\Lambda_\mathcal{A}}^{\dagger}(\lambda)\widehat{\Lambda_\mathcal{A}}(\lambda) + \sigma I(\lambda)\big]^{-1}\widehat{\Lambda_\mathcal{A}}^{\dagger}(\lambda), \tag{107}$$

where $I(\lambda)$ is the identity operator and $\sigma$ is a small positive constant. Thus,

$$f'(h) \approx \mathcal{F}^{-1}\big(\widehat{W}^{\dagger}_{\mathrm{opt}}(\lambda)\widehat{(\mathcal{A}f)}^{\dagger}(\lambda)\big) \tag{108}$$

$$= \mathcal{F}^{-1}\big(\widehat{\Lambda_\mathcal{A}}(\lambda)\big[\widehat{\Lambda_\mathcal{A}}^{\dagger}(\lambda)\widehat{\Lambda_\mathcal{A}}(\lambda) + \sigma I(\lambda)\big]^{-1}\widehat{(\mathcal{A}f)}^{\dagger}(\lambda)\big), \tag{109}$$

which is a regularized linear least square approximation of $f'$.

For Radon and modified exponential Radon transforms with uniform attenuation, $\Lambda_\mathcal{A}$ is a $SO(2)$ invariant distribution. Hence, by the $SO(2)$ invariance properties of the Fourier transform over $M(2)$, $\widehat{\Lambda_\mathcal{A}}$ is rank one. Then, Eq. (105) can be simplified as

$$\widehat{(\mathcal{A}f)}_{mn}(\lambda) = \overline{\tilde{f}_m(-\lambda)}\widehat{\Lambda_{\mathcal{A}}}_{0n}(\lambda), \tag{110}$$

where $\tilde{f}_m(\lambda)$ is the spherical harmonic decomposition of the standard Fourier transform of $f$. For $\mathcal{A} = \mathcal{T}'_\mu$, $\widehat{(\mathcal{T}'_\mu f)}_{mn}(\lambda)$ and $\widehat{\Lambda}_{\mathcal{T}'_\mu 0n}(\lambda)$ are given by

$$\widehat{(\mathcal{T}'_\mu f)}_{mn}(\lambda) = \frac{1}{\lambda^{n-m+1}}\Big[\widetilde{(\mathcal{T}'_\mu f)}_{-m}\big(\sqrt{\lambda^2+\mu^2}\big)\big(-\mu+\sqrt{\lambda^2+\mu^2}\big)^{n-m} + \widetilde{(\mathcal{T}_\mu f)}_{-m}\big(-\sqrt{\lambda^2+\mu^2}\big)\big(-\mu-\sqrt{\lambda^2+\mu^2}\big)^{n-m}\Big], \quad (111)$$

$$\widehat{\Lambda}_{\mathcal{T}'_\mu mn}(\lambda) = \delta_m \lambda^{-n-1}\Big((-1)^n\big[\big(\sqrt{\mu^2+\lambda^2}+\mu\big)^n\big] + \big[\big(\sqrt{\mu^2+\lambda^2}-\mu\big)^n\big]\Big). \quad (112)$$

Here, $\widetilde{(\mathcal{T}_\mu f)}_m(\sigma)$ denotes the circular harmonic decomposition of the one-dimensional standard Fourier transform of $(\mathcal{T}_\mu f)(\theta, r)$:

$$\widetilde{(\mathcal{T}_\mu f)}_m(\sigma) = \int_{S^1} \widetilde{(\mathcal{T}_\mu f)}(\boldsymbol{\omega}, \sigma) S_m(\boldsymbol{\omega})\, d(\boldsymbol{\omega}), \quad (113)$$

where

$$\widetilde{(\mathcal{T}_\mu f)}(\theta, \sigma) = \int_{\mathbb{R}} (\mathcal{T}_\mu f)(\theta, r) \mathrm{e}^{-\mathrm{i}\sigma r}\, dr. \quad (114)$$

Substitution of $\widehat{(\mathcal{T}'_\mu f)}_{mn}(\lambda)$ and $\widehat{\Lambda}_{\mathcal{T}'_\mu 0n}(\lambda)$ into Eq. (110) gives the following relationship between $f$ and $(\mathcal{T}_\mu f)$ (Yarman and Yazici, 2005a, 2005b)

$$\tilde{f}_{-m}(\lambda) = \widetilde{(\mathcal{T}_\mu f)}_{-m}\big(\sqrt{\lambda^2+\mu^2}\big) \times \frac{\lambda^m(-\mu+\sqrt{\lambda^2+\mu^2})^{n-m}}{(-1)^n(\sqrt{\mu^2+\lambda^2}+\mu)^n + (\sqrt{\mu^2+\lambda^2}-\mu)^n} + \widetilde{(\mathcal{T}_\mu f)}_{-m}\big(-\sqrt{\lambda^2+\mu^2}\big) \times \frac{\lambda^m(-\mu-\sqrt{\lambda^2+\mu^2})^{n-m}}{(-1)^n(\sqrt{\mu^2+\lambda^2}+\mu)^n + (\sqrt{\mu^2+\lambda^2}-\mu)^n}, \quad (115)$$

for any integer $n$. For $\mu = 0$, Eq. (115) gives the spherical harmonic decomposition of the projection slice theorem (Yarman and Yazici, 2005c).

Hence, as long as $\widehat{\Lambda}_{\mathcal{A}0n}(\lambda) \neq 0$, $k \in \mathbb{Z}$, a simplified inversion formula can be obtained as

$$f(\boldsymbol{x}) = \mathcal{F}^{-1}\big(\delta_m \tilde{f}_n(-\lambda)\big) = \overline{\left(\frac{\widehat{(\mathcal{A}f)}_{nk}(\lambda)}{\widehat{\Lambda}_{\mathcal{A}0k}(\lambda)}\right)}. \quad (116)$$

Numerical inversion of the Radon and exponential Radon transforms based on Eq. (108) will be presented in Section VI.E. Inversion methods based on the simplified Eqs. (110) and (116), are presented in Yarman and Yazici (2005a, 2005b, 2005c).

For the modified angle-dependent exponential Radon transform neither $f'$ nor $\Lambda_{\mathcal{T}'_\mu(\vartheta)}$ are $SO(2)$ invariant. Therefore, Eq. (106) or Eq. (108) has to be used to recover $f'$.

Assuming that $\mu$ is known, $f$ can be recovered from $f'$ by

$$f(\boldsymbol{x}) = \int_{SO(2)} f'(R_\phi, \boldsymbol{x})\, d(R_\phi). \tag{117}$$

In the next section, we present numerical reconstruction algorithms based on Eq. (108).

## *D. Numerical Algorithms*

### 1. *Fourier Transform over M(2)*

The computational complexity of the inversion algorithms is directly related to the computational complexity of the Fourier transform over $M(2)$. After reordering the integrals, the Fourier coefficients $\hat{f}_{mn}(\lambda)$ of $f$ over $M(2)$ can be expressed as follows:

$$\int_{S^1} \left( \int_{SO(2)} \left( \int_{\mathbb{R}^2} f(R_\theta, \boldsymbol{r}) e^{i\lambda \boldsymbol{r}\cdot\boldsymbol{\omega}}\, d\boldsymbol{r} \right) \overline{S_m(R_\theta^{-1}\boldsymbol{\omega})}\, d(\theta) \right) S_n(\boldsymbol{\omega})\, d(\boldsymbol{\omega}). \tag{118}$$

Choosing $S_n$ as the complex exponentials, that is, $S_n(\omega) = e^{in\omega}$, Eq. (118) can be performed in four consecutive standard Fourier transforms. For a detailed description of the Fourier transform algorithm over $M(2)$ based on Eq. (118), we refer to Kyatkin and Chirikjian (2000) and Yarman and Yazici (2003, 2005c).

If there are $\mathcal{O}(K)$ number of samples in each of $SO(2)$ and $\mathbb{R}$, the computational complexity of the Fourier transform implementation over $M(2)$ described above is $\mathcal{O}(K^3 \log K)$. If the projections and the unknown function do not depend on the $r_2$ component and $SO(2)$, computation complexity of the Fourier coefficients of the projections and the inverse Fourier transform of $\hat{f}_{mn}(\lambda)$ reduces to $\mathcal{O}(K^2 \log K)$.

2. *Reconstruction Algorithm*

The proposed inversion algorithm can be implemented in four steps as shown in the following diagram:

$$\begin{array}{ccccc} f & \xrightarrow{\mathcal{A}} & \mathcal{A}f & \xrightarrow[1]{\mathcal{F}} & \widehat{\mathcal{A}f} \\ \nwarrow^{4} \int_{SO(2)} & & & & \Big\downarrow 2\ \widehat{W}_{\text{opt}}(\lambda) \\ & & f' & \xleftarrow[3]{\mathcal{F}^{-1}} & \hat{f}' \end{array} \tag{119}$$

Let $f(\boldsymbol{x}) = 0$ for $|\boldsymbol{x}| > a$ and hence $\mathcal{A}f(\theta, r_1) = 0$ for $|r_1| > a$. The four-step reconstruction algorithm can be implemented as follows:

1. Compute the Fourier transform of $\widehat{\mathcal{A}f}$ of the projections over $M(2)$ for $m, n = 0, \pm 1, \ldots, \pm K$, and $\lambda = \frac{k\lambda_0}{K+1}$, $k = 0, \ldots, K$, for some $\lambda_0 > 0$.
2. For each $\lambda$, let $[\widehat{\Lambda_{\mathcal{A}}}(\lambda)]$, $[\widehat{\mathcal{A}f}(\lambda)]$, and $[\hat{f}'(\lambda)]$ denote the $2K-1$ by $2K-1$ matrix representations of the Fourier transforms of $\Lambda_{\mathcal{A}}$, $\mathcal{A}f$, and $f'$ over $M(2)$, respectively. Then, the Fourier transform of $f'$ over $M(2)$ can be approximated as

$$\big[\hat{f}'(\lambda)\big] \approx \big[\widehat{\Lambda_{\mathcal{A}}}(\lambda)\big]\Big(\overline{\big[\widehat{\Lambda_{\mathcal{A}}}(\lambda)\big]}^{T}\big[\widehat{\Lambda_{\mathcal{A}}}(\lambda)\big] + \sigma I\Big)^{-1}\overline{\big[\widehat{\mathcal{A}f}(\lambda)\big]}^{T}, \tag{120}$$

   where $\sigma$ is a positive constant close to zero; overline and superscript $T$ are the complex conjugation and transpose operations, respectively.
3. Take the inverse Fourier transform of $\hat{f}'_{mn}(\lambda)$ to obtain $f'$.
4. Integrate $f'$ over $SO(2)$ to recover $f$.

## *E. Numerical Simulations*

1. *Radon Transform*

The numerical implementation of the algorithm introduced in the previous subsection is performed on a two-dimensional modified Shepp–Logan phantom of size 129 × 129 pixels, generated by MATLAB's *phantom* function. The projections of the phantom are taken from 129 equally spaced angles over $2\pi$ and 129 parallel lines for each angle. To avoid aliasing, the image and the projections were zero-padded to 257 pixels in horizontal and vertical and radial directions. The Fourier transform over $M(2)$ was numerically implemented as described in Section VI.D and Yarman and Yazici (2003, 2005d). All the numerical implementations were performed using MATLAB. For comparison purposes, the standard filtered backprojection (FBP) method with Ram–Lak filter is used.

Figure 4a presents the reconstructed phantom image. For reconstruction, the regularization factor $\sigma$ is set to $10^{-5}$. The effect of the regularization term

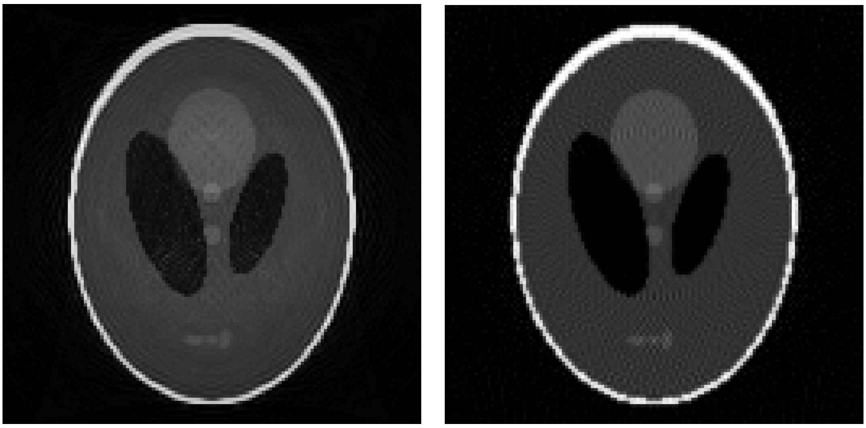

(a) *Proposed algorithm* (b) FBP

FIGURE 4. Reconstruction of the modified Shepp–Logan phantom from its Radon transform using proposed algorithms and FBP. (a) Reconstruction by proposed algorithm, for $\sigma = 10^{-8}$. (b) Reconstruction by FBP.

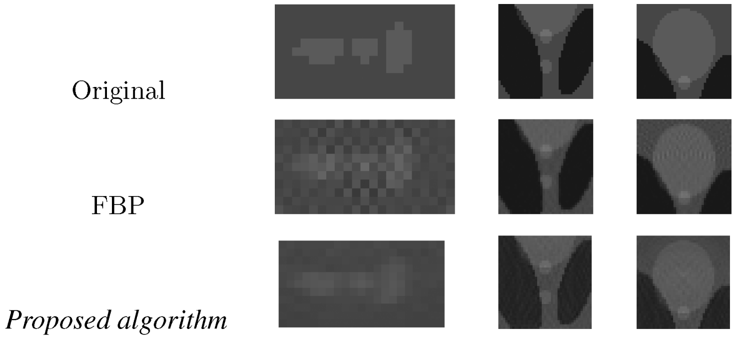


FIGURE 5. Comparison of details in reconstructed Shepp–Logan phantom from its Radon transform.

was discussed in Yarman and Yazici (2005d). For visual comparison, FBP reconstructed images are shown in Figure 4b. The details of the reconstructed images are shown in Figure 5. These results suggest that the proposed reconstruction algorithm produces details at least as good as that of the FBP algorithm.

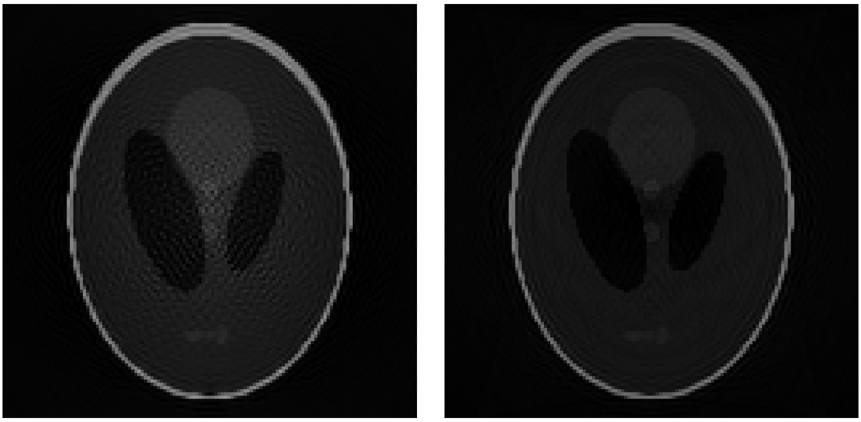

(a) (b)

FIGURE 6. Reconstruction of the modified Shepp–Logan phantom from its exponential Radon transform using the proposed algorithm for $\sigma = 10^{-10}$. Reconstructed images for (a) $\mu = 0.154\ \text{cm}^{-1}$ and (b) $\mu = \text{i}0.154\ \text{cm}^{-1}$.

### 2. *Exponential Radon Transform with Uniform Attenuation*

Numerical simulations are performed on a two-dimensional modified Shepp–Logan phantom image corresponding to a region of $13.1 \times 13.1\ \text{cm}^2$, discretized by $129 \times 129$ pixels. The projections of the phantom are taken from 129 equally spaced angles over $2\pi$ and 129 parallel lines for each angle. The Fourier transform over $M(2)$ was numerically implemented as previously described. All numerical implementations were performed using MATLAB. The regularization factor $\sigma$ is set to $10^{-10}$. Taking $\mu = 0.154\ \text{cm}^{-1}$ and $\mu = \text{i}0.154\ \text{cm}^{-1}$, the reconstructed images using the proposed algorithm is presented in Figure 6. An extensive study on the proposed reconstruction algorithm and numerical experiments can be found in Yarman and Yazici (2005b).

The numerical simulations demonstrate the applicability and the performance of the proposed inversion algorithm. Note that further improvements in reconstruction can be achieved by improving the numerical implementation of the Fourier transform over $M(2)$.

## VII. CONCLUSION

In this chapter, we introduced a MMSE solution for the deconvolution problems formulated over groups using the group representation theory and the concept of group stationarity. We used these concepts to address the receiver and waveform design problems in wideband extended range-Doppler imaging and the inversion of the Radon and exponential Radon transforms for the transmission and emission tomography.

We treated the wideband radar/sonar echo signal as the Fourier transform of the range-Doppler extended target reflectivity function with respect to the affine group evaluated at the transmitted pulse. The clutter filtering and target reconstruction naturally couples with the design of transmitted pulses. We developed a Wiener filtering method in the Fourier transform of the affine group to remove clutter. This treatment leads to a framework that simultaneously addresses multiple problems, including joint design of transmission and reception strategy, suppression of clutter, and use of a priori information.

We presented convolution representation of the Radon and exponential Radon transforms. The convolution representations are block diagonalized in the Fourier domain of the Euclidean motion group. Due to the rotation invariance properties of the Fourier transform of the unknown image over the Euclidean motion group, the block diagonal representation is further simplified to a diagonal form. We introduced a new algorithm for the inversion of these transforms and demonstrated their performance in numerical examples.

The fundamental results introduced here are applicable to other imaging problems that can be formulated as convolutions over groups. Such problems include inverse rendering (Ramamoorthi and Hanrahan, 2001), omnidirectional image processing (Makadia *et al.*, 2005), and inversion of other integral transforms of transmission and emission tomography (Yarman and Yazici, 2005e).

## ACKNOWLEDGMENTS

This material is based partly on research sponsored by the U.S. Air Force Research Laboratory, under agreement No. FA9550-04-1-0223. The U.S. Government is authorized to reproduce and distribute reprints for governmental purposes notwithstanding any copyright notation thereon.

## APPENDIX A

### *Definitions*

Definitions of the basic concepts used in this chapter are provided for readers' convenience. Detailed discussions and rigorous treatment of these concepts can be found in Milies and Sehgal (2002), Groove (1997), and Onishchik (1993).

*Definition A1.1*

- Let $G$ be a group, $F$ a field, and $V$ a vector field over $F$. A *representation* of a group $G$ is a homomorphism $\rho$ from $G$ into the group of automorphisms of $V$, denoted by $GL(V)$, that is, $\rho : G \to GL(V)$, such that $\rho(g) = \rho_g$.
- If $V$ is a $n$-dimensional vector space over $F$, then for a fixed basis of $V$ there is an isomorphism $\varphi$ from $GL(V)$ into $GL(n, F)$. Therefore, $\varphi$ induces another representation $(\varphi \circ \rho)$ of $G$ into $GL(n, F)$, which is called a matrix representation. Any representation of $G$ into $GL(V)$ is equivalent to a representation into $GL(n, F)$ and vice versa. The integer $n$ is called the *degree* of $\rho$.

*Definition A1.2*

- Let $W$ be a subspace of $V$. If for all elements $g \in G$, $\rho_g v$ is again in $W(\rho_g W \subset W)$, then $W$ is said to be *invariant* under $\rho$ or, equivalently, *$\rho$-invariant*. If $V$ is nonempty and has no proper $\rho$-invariant subspace $W$, then the representation is said to be *irreducible*, else *reducible*.
- A group $G$ is called a *topological group* if $G$ is a topological space satisfying the Hausdorff separation axiom and the mapping $(x, y) \to xy^{-1}$ is a continuous mapping from $G \times G$ into $G$.
- Let $G$ be a topological group. A *unitary representation* of $G$ over a Hilbert space $H$ is a strongly continuous homomorphism $U$ from $G$ into the group of unitary operators of $H$, $U(H)$. $H$ is called the representation space of $U$ and denoted by $H(U)$. The dimension of $H(U)$ is the called the degree of $U$.
- Let $W$ be a subspace of a representation space $H(U)$ of a unitary representation $U$. Then $W$ is said to be *invariant* under $U$ if $U(g)W \subset W$ for all $g \in G$. A unitary representation $U$ is called *irreducible* if $H(U)$ is nonempty and has no proper subspace invariant under $U$.
- Let $G$ be a locally compact topological group and let $H(R) = L^2(G, dg)$ be the Hilbert space of square-integrable functions on $G$ with respect to right Haar measure on $G$. Let $f$ be a function in $H(R)$. Define the operator $R$ on $H(R)$ by $[R(g)f](h) = f(hg)$. Then $R$ is a unitary representation of $G$ and is called the *right regular representation* of $G$. Similarly, the *left regular representation* $L$ is defined by $[L(g)f](h) = f(g^{-1}h)$.

*Definition A1.3*

- Let $G$ be a group, and let $K$ be a subgroup of $G$. Given an element $g \in G$, the subsets of the form

$$gK = \{gk\colon\ k \in K\}, \qquad Kg = \{kg\colon\ k \in K\}$$

are called the *left* and *right cosets* of the subgroup $K$ determined by $g$. The equivalence class of the cosets are denoted by $G/K$ and $K\backslash G$, respectively.

- $G$ acts on the set $K\backslash G$ by right multiplications, and since it is an automorphism of the group $K\backslash G$, it also induces automorphism over the representations of $K\backslash G$. Hence, this automorphism induces a representation of $G$ over the complex-valued function over $K\backslash G$ called the *quasi-right regular representation*.

## APPENDIX B

### *Distributions and Fourier Transform Over $M(2)$*

Let $\mathcal{D}(M(2))$ denote the space of compactly supported functions on $M(2)$; and $\mathcal{S}(M(2))$ denote the space of rapidly decreasing functions on $M(2)$. The Fourier transform over $M(2)$ can be extended to $\mathcal{D}(M(2))$ and $\mathcal{S}(M(2))$, on $M(2)$, and is injective (Sugiura, 1975). Let $\mathcal{D}'(M(2))$ and $\mathcal{S}'(M(2))$ denote the space of linear functionals over $\mathcal{D}(M(2))$ and $\mathcal{S}(M(2))$, respectively. $\mathcal{D}'(M(2))$ and $\mathcal{S}'(M(2))$ are called the space of distributions and tempered distributions over $M(2)$ and $\mathcal{S}'(M(2)) \subset \mathcal{D}'(M(2))$. Let $u \in \mathcal{D}'(M(2))$ and $\varphi \in \mathcal{D}(M(2))$. The value $u(\varphi)$ is denoted by $\langle u, \varphi\rangle$ or $\int_{M(2)} u(g)\varphi(g)\,dg$, similarly for $u \in \mathcal{S}(M(2))$.

Let $\varphi \in \mathcal{S}(M(2))$ and $u \in \mathcal{S}'(M(2))$. The Fourier transform $\hat{u}$ of $u$ over $M(2)$ is defined by $\langle \hat{u}, \widehat{\varphi}\rangle = \langle u, \varphi\rangle$.

Let $u$ and $v$ be two distributions, at least one of which has compact support. Then the convolution of $u$ and $v$ is a distribution that can be computed using either of the following

$$\langle u * v, \varphi\rangle = \big\langle u(h), \big\langle v(g), \varphi(hg)\big\rangle\big\rangle = \big\langle v(g), \big\langle u(h), \varphi(hg)\big\rangle\big\rangle. \tag{B.1}$$

If either of $u$ or $v$ is a tempered distribution and the other is compactly supported, then $u * v$ is a tempered distribution. Without loss of generality, assume that $u$ is compactly supported and $v \in \mathcal{S}'(M(2))$. Then $\hat{u}$ can be computed by

$$\hat{u} = \big\langle u(g), U_{mn}\big(g^{-1}, \lambda\big)\big\rangle. \tag{B.2}$$

Using Eqs. (B.1) and (B.2), the Fourier transform of the convolution $u * v$ over $M(2)$ is obtained to be

$$\mathcal{F}(u * v) = \sum_k \hat{v}_{mk}(\lambda)\hat{u}_{kn}(\lambda). \tag{B.3}$$

## REFERENCES

Abramowitz, M., Stegun, I.A. (1972). *Orthogonal Polynomials*. Dover, New York. Chap. 22, pp. 771–802.

Artin, M. (1991). *Algebra*. Prentice-Hall, Englewood Cliffs, NJ.

Barrett, H.H. (1984). The Radon transform and its applications. *Progress in Optics* **21**, 271–286.

Bellini, S., Piancentini, M., Cafforio, C., Rocca, F. (1979). Compensation of tissue absorption in emission tomography. *IEEE Transactions on Acoustics, Speech and Signal Processing* **ASSP-27**, 213–218.

Blahut, R.E. (1991). *Algebraic Methods for Signal Processing and Communications Coding*. Springer-Verlag, New York.

Chirikjian, G.S., Ebert-Uphoff, I. (1998). Numerical convolution on the Euclidean group with applications to workspace generation. *IEEE Trans. Robotics Automat.* **14**, 123–136.

Cook, C.E., Bernfeld, M. (1967). *Radar Signals*. Academic, New York.

Cormack, A.M. (1963). Representation of a function by its line integrals with some radiological applications. *Journal of Applied Physics* **34**, 2722–2727.

Cormack, A.M. (1964). Representation of a function by its line integrals with some radiological applications II. *Journal of Applied Physics* **35**, 2908–2913.

Deans, S.R. (1983). *The Radon Transform and Some of Its Applications*. Wiley, New York.

Diaconis, P. (1988). *Group Representations in Probability and Statistics*. *Institute of Mathematical Statistics Monograph*, vol. 11. Inst. Math. Statist., Hayward, CA.

Duflo, M., Moore, C.C. (1976). On the regular representation of a nonunimodular locally compact groups. *J. Funct. Anal.* **21**, 209–243.

Ebert-Uphoff, I., Chirikjian, G.S. (1996). Inverse kinematics of discretely actuated hyper redundant manipulators using workspace density. In: *Proc. of IEEE Int. Conf. Robotics and Automation, Minneapolis, MN*, pp. 139–145.

Ferraro, M. (1992). Invariant pattern representations and Lie group theory. In: *Advances in Electronics and Electron Physics*, vol. 84. Academic, New York, pp. 131–196.

Gelfand, I.M., Graev, M.I., Vilenkin, N.J. (1966). *Generalized Functions, Integral Geometry and Representation Theory, vol. 5*. Academic Press, New York.

Gelfand, I.M., Shilov, G.E. (1964). *Generalized Functions, Properties and Operations, vol. 1*. Academic Press, New York.

Groove, L.C. (1997). *Groups and Characters*. Wiley, New York.

Hannan, E.J. (1965). *Group Representations and Applied Probability. Methuens Review Series in Applied Probability*, vol. 3. Methuen & Co., Ltd., London, U.K.

Hawkins, G.W., Leichner, P.K., Yang, N.-C. (1988). The circular harmonic transform for SPECT reconstruction and boundary conditions on the Fourier transform on the sinogram. *IEEE Transactions on Medical Imaging* **7**, 135–148.

Helgason, S. (1999). *The Radon Transform*, 2nd ed. Birkhäuser, Boston, MA.

Helgason, S. (2000). *Groups and Geometric Analysis: Integral Geometry Invariant Differential Operators and Spherical Functions*. American Mathematical Society, Providence, RI.

Inouye, T., Kose, K., Hasegawa, A. (1989). Image reconstruction algorithm for single-photon-emission computed tomography with uniform attenuation. *Phys. Med. Biol.* **34**, 299–304.

Kanatani, K. (1990). *Group Theoretical Methods in Image Understanding*. Springer-Verlag.

Kuchment, P., Shneiberg, I. (1994). Some inversion formulas in the single photon emission computed tomography. *Applicable Analysis* **53**, 221–231.

Kyatkin, A.B., Chirikjian, G.S. (1998). Regularized solution of a nonlinear convolution equation on the Euclidean group. *Acta Applicandae Mathematicae* **53**, 89–123.

Kyatkin, A., Chirikjian, G. (2000). Algorithms for fast convolutions on motion groups. *Applied Computational Harmonic Analysis* **9**, 220–241.

Lenz, R. (1990). *Group Theoretical Methods in Image Processing*. *Lecture Notes in Computer Science*. Springer-Verlag, Berlin, Germany.

Makadia, A., Geyer, C., Daniilidis, K. (2005). Radon-based structure from motion without correspondences. In: *Proceedings of CVPR 2005*.

Metz, C., Pan, X. (1995). A unified analysis of exact methods of inverting the 2-D exponential Radon transform, with implications for noise control in SPECT. *IEEE Transactions on Medical Imaging* **14**, 643–658.

Milies, C.P., Sehgal, S.K. (2002). *An Introduction to Group and Rings*. Kluwer, Norwell, MA.

Miller, W. (1991). Topics in harmonic analysis with applications to radar and sonar. In: Blahut, R.E., Miller, W., Wilcox, C.H. (Eds.), *Radar and Sonar. Part I*, *IMA Volumes in Mathematics and Its Applications*. Springer-Verlag, New York, pp. 66–168.

Naimark, M.A. (1959). *Normed Rings*. Noordhoff N.V., Groningen, The Netherlands.

Naparst, H. (1991). Dense target signal processing. *IEEE Trans. Inform. Theory* **37**, 317–327.

Nathanson, F., Reilly, J., Cohen, M. (1999). *Radar Design Principles—Signal Processing and the Environment*. SciTech Publishing.

Natterer, F. (1986). *The Mathematics of Computerized Tomography*. Wiley–Teubner, New York.

Onishchik, A.L. (1993). *Lie Groups and Lie Algebras I*. Springer-Verlag, New York.

Pintsov, D.A. (1989). Invariant pattern recognition, symmetry and the Radon transforms. *J. Opt. Soc. Amer.* **6**, 1545–1554.

Popplestone, R. (1984). Group theory in robotics. In: Brady, M., Paul, R. (Eds.), *Proc. Robotics Research: The 1st Int. Symp*. MIT Press, Cambridge, MA.

Puro, A. (2001). Cormack-type inversion of exponential Radon transform. *Inverse Problems* **17**, 179–188.

Radon, J. (1917). Über die Bestimmung von Funktionen durch ihre Integralwerte längs gewisser Männigfaltigkeiten. *Berichte Sächsische Akademie der Wissenschaften Leipzig. Math.-Phys. Kl.* **69**, 262–267.

Ramamoorthi, R., Hanrahan, P. (2001). A signal processing framework for inverse rendering. In: *Proc. 28th Annu. Conf. Computer Graphics and Interactive Techniques (SIGGRAPH)*, pp. 117–128.

Rebollo-Neira, L., Pastino, A., Fernandez-Rubio, J. (1997). Frames: A maximum entropy statistical estimate of the inverse problem. *Journal of Mathematical Physics* **38**, 4863–4871.

Rebollo-Neira, L., Pastino, A., Fernandez-Rubio, J. (2000). Reconstruction of the joint time-delay Doppler-scale reflectivity density in the wideband regime: A frame theory based approach. *Journal of Mathematical Physics* **41**, 5325–5341.

Rouviére, F. (2001). Inverting Radon transforms: The group theoretic approach. *L'Enseignement Mathématique* **47**, 205–252.

Sattinger, D.H., Weaver, O.L. (1986). *Lie Groups and Algebras with Applications to Physics, Geometry and Mechanics*. Springer-Verlag, New York.

Seeley, R.T. (1966). Spherical harmonics. *The American Mathematical Monthly* **73**, 115–121.

Srivastava, H.M., Buschman, R.G. (1977). *Convolution Equation, with Special Function Kernels*. Wiley, New York.

Strichartz, R.S. (1981). $L^p$ estimates for Radon transforms in Euclidean and non-Euclidean spaces. *Duke Mathematical Journal* **48**, 699–727.

Sugiura, M. (1975). *Unitary Representations and Harmonic Analysis*. Kodansha, Tokyo.

Swick, D.A. (1969). A review of wideband ambiguity functions. NRL Rep. 6994. Tech. Rep., Naval Research Laboratory, Washington, DC.

Taylor, J. (1995). *Introduction to Ultra-wideband Radar Systems*. CRC Press, Florida.

Tewfik, A.H. (1987). *Recursive Estimation and Spectral Estimation for 2-d Isotropic Random Fields*. Ph.D. thesis, MIT, Cambridge, MA.

Tikhonov, A.N., Arsenin, V.Y. (1977). *Solutions of Ill-Posed Problems*. Wiley, New York.

Tretiak, O., Metz, C. (1980). The exponential Radon transform. *SIAM J. Appl. Math.* **39**, 341–354.

Vilenkin, N.J. (1988). *Special Functions and the Theory of Representations*. American Mathematical Society, Providence, RI.

Volchkov, V. (2003). *Integral Geometry and Convolution Equations*. Kluwer Academic Publishers, Dordrecht; Boston, MA.

Weiss, L.G. (1994). Wavelets and wideband correlation processing. *IEEE Signal Processing Mag.* **11**, 13–32.

Yadrenko, M.I. (1983). *Spectral Theory of Random Fields*. *Translation Series in Mathematics and Engineering*. Optimization Software Inc./Springer-Verlag, New York.

Yaglom, A.M. (1961). Second order homogeneous random fields. In: *Proc. 4th Berkley Symp. Mathematical Statistics and Probability, vol. 2*. Univ. Calif. Press, Berkeley, CA, pp. 593–622.

Yarman, C., Yazici, B. (2003). Radon transform inversion via Wiener filtering over the Euclidean motion group. In: *Proceedings of IEEE International Conference on Image Processing 2003, vol. 2, Barcelona, Spain*, pp. 811–814.

Yarman, C.E., Yazici, B. (2005a). Exponential Radon transform inversion based on harmonic analysis of the Euclidean motion group. In: *Proceedings of IEEE International Conference on Image Processing 2005*.

Yarman, C.E., Yazici, B. (2005b). Exponential Radon transform inversion based using harmonic analysis of the Euclidean motion group. Preprint.

Yarman, C.E., Yazici, B. (2005c). Radon transform inversion based on harmonic analysis of the Euclidean motion group. In: *Proceedings of IEEE International Conference on Acoustics, Speech, and Signal Processing 2005*.

Yarman, C.E., Yazici, B. (2005d). Radon transform inversion based on the harmonic analysis of the Euclidean motion group. Preprint.

Yarman, C.E., Yazici, B. (2005e). Reconstructive integral transforms of transmission and emission tomography as convolutions over the Euclidean motion group. Preprint.

Yazici, B. (1997). Group invariant methods in signal processing. In: *Proc. Conf. Information Sciences and Systems, Baltimore, MD*, pp. 185–189.

Yazici, B. (2004). Stochastic deconvolution over groups. *IEEE Transactions on Information Theory* **50**, 494–510.

Yazici, B., Izzetoglu, M. (2002). Optimal Wiener filtering for self-similar processes. In: *Proc. of Int. Conf. Acoustics Speech and Signal Processing, vol. 2*, pp. 1697–1700.

Yazici, B., Izzetoglu, M., Onaral, B., Bilgutay, N. (2001). Kalman filtering for self-similar processes. In: *Proc. IEEE 11th Int. Workshop on Statistical Signal Processing*, pp. 82–85.

Yazici, B., Kashyap, R.L. (1997). Second order stationary, self-similar models for 1/f processes. *IEEE Trans. Signal Processing* **45**, 396–410.

Yazici, B., Xie, G. (2005). Wideband extended range-Doppler imaging and diversity waveform design. *IEEE Transactions on Information Theory*, submitted for publication.